JACS
JOURNAL OF THE AMERICAN CHEMICAL SOCIETY
pubs.acs.org/JACS
Perspective

Mind the Gap: The Role of Mass Transfer in Shaped Nanoporous Adsorbents for Carbon Dioxide Capture

Margot F. K. Verstreken, Nicolas Chanut,* Yann Magnin, Héctor Octavio Rubiera Landa, Joeri F. M. Denayer, Gino V. Baron, and Rob Ameloot*

Cite This: https://doi.org/10.1021/jacs.4c03086
Read Online

ABSTRACT: Adsorptive separations by nanoporous materials are major industrial processes. The industrial importance of solid adsorbents is only expected to grow due to the increased focus on carbon dioxide capture technology and energy-efficient separations. To evaluate the performance of an adsorbent and design a separation process, the adsorption thermodynamics and kinetics must be known. However, although diffusion kinetics determine the maximum production rate in any adsorption-based separation, this aspect has received less attention due to the challenges associated with conducting diffusion measurements. These challenges are exacerbated in the study of shaped adsorbents due to the presence of porosity at different length scales. As a result, adsorbent selection typically relies mainly on adsorption properties at equilibrium, i.e., uptake capacity, selectivity and adsorption enthalpy. In this Perspective, based on an extensive literature review on mass transfer of CO_2 in nanoporous adsorbents, we discuss the importance and limitations of measuring diffusion in nanoporous materials, from the powder form to the adsorption bed, considering the nature of the process, i.e., equilibrium-based or kinetic-based separations. By highlighting the lack of and discrepancies between published diffusivity data in the context of CO_2 capture, we discuss future challenges and opportunities in studying mass transfer across scales in adsorption-based separations.

IMPORTANCE OF MASS TRANSFER IN INDUSTRIAL ADSORPTION PROCESSES

It is estimated that separation and purification of chemicals accounts for 10−15% of the world's energy consumption.[1] Shifting away from energy-intensive distillation and absorption processes would bring down operational costs and help to meet midterm greenhouse gas emissions targets.[2,3] Nanoporous materials may play a key role in this transition by enabling adsorption-based separation processes that have a lower energy demand and can be electrified with green power.[2] Established adsorption-based separation processes include air separation, natural gas sweetening, and selected hydrocarbon separations.[3] The industrial importance of solid adsorbents is only expected to grow due to an increased focus on carbon dioxide (CO_2) capture and utilization,[4−6] alkene/alkane separations for the manufacturing of plastics,[7−10] etc.

In contrast to technologies like distillation that operate under steady-state conditions, adsorption-based separation technologies involve transient operations, i.e., adsorption/desorption cycles are carried out on multiple adsorbent beds. Once an adsorption cycle is completed and the first component to break through has been recovered at high purity, a regeneration step is performed to recover the more strongly adsorbed one, generally at a lower purity due to the presence of the coadsorbed species. In such processes, the sequence of breakthrough and the achievable product purities are governed by an interplay of mixture adsorption equilibria and intracrystalline diffusion inside the porous adsorbent.[11]

Generally, adsorption-based separations can be classified into two categories: (i) equilibrium separations, where the separation process is driven by the difference in thermodynamic affinities of the adsorbates for the solid adsorbent, and, (ii) kinetic separations, which exploit differences in mass transport rates of the adsorbates in the pores of the adsorbent. In equilibrium separations, the adsorbent should have a high thermodynamic selectivity and uptake capacity for one of the components, fast mass transfer is needed as it enables fast cycling operations resulting in higher overall productivity. While the uptake capacity is the quantity typically measured in the laboratory, it is more important for the application of an adsorbent to look at the working capacity, i.e., the difference between amounts adsorbed under adsorption and desorption conditions, pressures in a Pressure Swing Adsorption (PSA) process or temperatures in a Temperature Swing adsorption process (TSA). This quantity is therefore not only adsorbent-dependent but also depends on the separation task considered. The selection of the adsorbent should be made with the application in mind. In kinetic separations, an adsorbent should have a high working capacity and kinetic selectivity for one of the components. Ideally, the component to be recovered would be the one that diffuses more slowly into the micropores (d < 2 nm, following the IUPAC classification,[12] with d the pore diameter) of the adsorbent.

Received: March 1, 2024
Revised: August 5, 2024
Accepted: August 6, 2024

https://doi.org/10.1021/jacs.4c03086
J. Am. Chem. Soc. XXXX, XXX, XXX−XXX

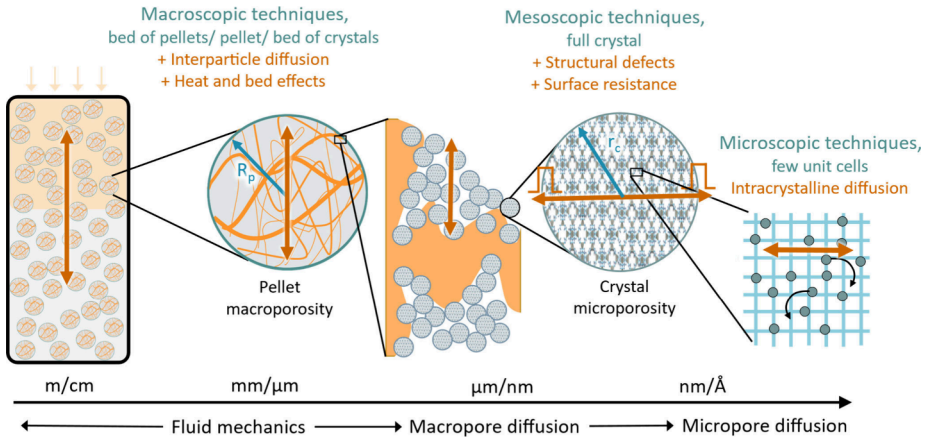

Figure 1. Schematic illustration of different pore scales involved in an arbitrary adsorbent-based separation process in relation to the different diffusional length scales and their corresponding mass transfer processes and experimental techniques. (Left to right) A column made of pellets, one pellet (Rp pellet radius) and its intraporosity, crystals forming the pellet and interparticle porosity, one crystal (r_c crystal radius) and its intraporosity, and gas molecules moving in a crystal.

It will only slowly enter the adsorbent compared to the other adsorbates, and hence, will break through first, resulting in a high-purity stream. In both types of separation, the affinity of the adsorbent for the adsorptive (i.e., the adsorption enthalpy) must be taken into account as well—while higher adsorption enthalpy generally leads to higher equilibrium selectivity, it also results in more energy-intensive regeneration and the exothermic nature of adsorption becomes more pronounced. Similar heat generation and adsorbent regeneration considerations for the faster diffusing component also apply to kinetic separations.

In practice, equilibrium separations are more frequently applied than kinetic separations since precisely matching the contact time between the gas mixture and the adsorbent to the mass transfer rate of the adsorptive is more challenging at an industrial scale. For example, in fixed-bed adsorbers with contact times that are too long or adsorbent particles that are too small, the kinetic selectivity would be lost as the system approaches equilibrium, but if the contact time is too short, the bed capacity would not be fully employed. However, in many cases, the equilibrium selectivity is limited, and the required purity levels cannot be reached through thermodynamic separation. Even for molecules with a similar equilibrium uptake, nanoporous materials enable very large differences in adsorption rates.[13] In these complex, yet often critical separations, kinetically driven separations can be of strong interest.[14] Examples of equilibrium-based adsorptive separations include hydrogen production,[15−17] carbon capture,[18−20] hydrocarbons separation and purification,[21−23] and air separation,[24,25] among other industrially relevant separation operations.[26] Yet, their kinetically controlled counterparts, have been successful in specific cases as well, including CO_2/CH_4 separation with carbon molecular sieve materials,[27] separation of N2 from air,[28,29] removal of N_2 from natural gas using Engelhard titanosilicates,[30] and the separation of linear paraffin streams using zeolite 5A.[31]

A wide variety of nanoporous materials has been studied in separation and purification processes, including zeolites,[32] activated carbons,[33] carbon molecular sieves (CMS),[34] metal−organic frameworks (MOFs),[35,36] silica-based materials,[37] and porous polymers.[38] These adsorbents are commonly synthesized in powder form and subsequently shaped into pellets, granules, extrudates, or monoliths for use in an adsorption bed.[39−41] This might require mixing the powder with a binder, to provide the required mechanical properties for utilization in an adsorption bed. Consequently, several mass transfer resistances are present at different length scales. Since the vast majority of materials discussed in this Perspective are crystalline (i.e., zeolites and MOFs), we refer to the primary adsorbent particles as 'crystals'. Correspondingly, we refer to the shaped adsorbent as "pellets". In the crystals, intraparticle diffusion or surface barriers can control the transport of the guest species[42−44] (Figure 1). At the pellet scale, mass transfer resistances in the mesopores ($2\ \text{nm} \geq d \geq 50\ \text{nm}$) and macropores ($d > 50$ nm) surrounding the crystals and binder particles play a role as well. The largest mass transfer resistance dominates the overall (apparent) diffusional time constant of the adsorption process. Kinetic separations depend on differences in micropore diffusivities, which can be very large, with molecular sieving in zeolites and MOFs as the limiting case. On the other hand, in equilibrium separations, reaching equilibrium faster enables shorter cycle times, and, hence minimal mass transfer resistances are desired.[39,45−47] In other words, adsorption equilibrium should be established quickly in the crystals, and the characteristic diffusion time would be determined by the meso/macroporous resistance of the pellets. Because mass transfer determines the maximum production rate in all adsorption-based separations,[48] selecting adsorbents based on thermodynamic considerations alone may lead to unexpected and suboptimal results.[49−51] Gaining better insight into mass transfer is required for a fundamental understanding and is directly linked to equipment design and operation, system costs, and ultimately, the viability of an adsorption-based separation.

Equilibrium single-component measurements (i.e., using a single adsorbate) are routinely performed. In contrast, mass transfer measurements can be challenging, especially for fast-diffusing molecules. The scarcity and inconsistency of reported diffusivity values in the open literature underline the limitations of the current measurement techniques.[48,52] Therefore, based on an extensive overview of reported CO_2 diffusion data in nanoporous materials, the objective of this Perspective is to highlight common methods available to measure diffusivities and their limitations, and, identify target areas for further study. In the context of carbon capture, substantial research has been conducted on designing nano-

https://doi.org/10.1021/jacs.4c03086
J. Am. Chem. Soc. XXXX, XXX, XXX−XXX

porous materials for CO_2 capture and separation.[53−55] Nevertheless, as will become clear, significant gaps remain in our understanding of the mass transfer over the different scales at play, its predictability and the role of single-component data in multicomponent processes.

■ ASSESSING THE MASS TRANSFER BEHAVIOR OF A GAS−ADSORBENT PAIR

Introductory Concepts of Mass Transfer. Diffusion mechanisms in porous materials depend on the ratio of the molecule size σ to the pore diameter d. For a small molecule such as CO_2 diffusing in a large pore $\sigma \ll d$ (macropores), transport is dominated by convection and viscous diffusion. At this scale, intermolecular collisions dominate and interactions with the pore walls are negligible.[56] For smaller pore sizes (mesopores), the Knudsen diffusion regime prevails, in which the molecular mean free path is comparable to or larger than the pore diameter, with more frequent molecule-wall collisions than intermolecular collisions.[46] In pores with sizes of few molecular diameters (micropores), the diffusing molecules interact strongly with the pore walls and diffusion is an activated process;[57−59] the stronger the molecule-wall interaction, the slower the diffusion.[60,61] In such small pores, macroscopic parameters such as the fluid viscosity become meaningless and the continuum laws of fluid mechanics fail in describing molecular flows.[62,63]

Transport or Fickian diffusion through nanoporous materials can be described by Fick's laws.[47] Fick's first law expresses the diffusive flux, j, as a function of the molecule concentration gradient, $\nabla\rho$:

$$j = -D_t \nabla \rho \tag{1}$$

with D_t the Fickian or transport diffusion coefficient. This concentration-dependent parameter embeds porous network complexity, which includes pore sizes, texture, morphology and topology, the strength of fluid−solid interactions, and thermodynamic parameters such as temperature and pressure (i.e., concentration, which determines the loading). The conservation equation, Fick's second law of diffusion, can be derived from eq 1 and describes the relation between the rate of change of the concentration in a volume and the local curvature of the concentration gradient over that volume:

$$\frac{\partial \rho}{\partial t} = -\nabla .\ (D_t \nabla \rho) \tag{2}$$

In addition to transport diffusion, adsorbed molecules also diffuse in the absence of a concentration gradient, due to the random molecular motion that remains present at equilibrium. This behavior is described by the self-diffusion coefficient D_s.[47,64] Measuring these two types of diffusion coefficients requires different experimental approaches, which are discussed in the next section.

The transport diffusion coefficient can also be written as $D_t = D_0\,\Gamma$, with D_0 the corrected (also called collective) diffusion coefficient and Γ the thermodynamic factor (also called Darken's factor):

$$\Gamma = \frac{d(\ln(P))}{d(\ln(\rho))} \tag{3}$$

with P the pressure and ρ the adsorbate concentration in the adsorbent. Γ depends on the latter, ranging from one at infinite dilution to infinity at saturation, with an analytical form linked to the isotherm type ($\Gamma = (1 - \rho/\rho_s)^{-1}$ for a Langmuir shaped isotherm). For a more detailed explanation, readers are directed to consult the following publication.[65] The transport, or nonequilibrium diffusion is of relevance in separation processes. However, under diluted conditions (i.e., at low adsorbed concentrations) where molecules are free of collective interactions, $\Gamma \sim 1$ and the self-, corrected, and transport diffusion converge to a similar value and can be addressed as a fair estimate of one another, $D_s \sim D_0 \sim D_t$.

Analytical solutions of eq 2 were provided by Carslaw and Jaeger,[66] Crank,[67] and Yang,[68] for a wide range of adsorbent geometries under specific boundary conditions and restricted by several assumptions, i.e., a constant diffusion coefficient, implying dilute conditions or small pressure gradients (corresponding to a locally linear region of the isotherm). For detailed derivations, we direct the reader to these excellent books.[31,46,66−68]

Transforming adsorbent powders or crystals into a shaped body for process-scale applications leads to mass transfer resistances at different scales, including macropore and external particle film resistances. This is exemplified by the overall mass transfer coefficient expression for a bidispersed spherical pellet (i.e., consisting of a network of micropores accessible through the macropores) based on the linear driving force model (LDF):[20,39,69]

$$\frac{1}{k^{ldf}} = \frac{R_p}{3k_f}\frac{q^*}{c}\rho_p + \frac{R_p^2}{15\epsilon_p D_e}\frac{q^*}{c}\rho_p + \frac{r_c^2}{15D_c} \tag{4}$$

whereby the terms in the sum represent the external particle film resistance with coefficient, k_f; the macropore resistance with effective diffusivity, D_e; and the micropore resistance with crystal diffusivity, D_c; the (equilibrium) concentration of adsorbate in the fluid phase, q^*; the concentration of adsorbate in contact with the adsorbent, c; the pellet radius, R_p; the crystal radius, r_c, respectively. The pellet porosity, ϵ_p, and density, ρ_p, are required to quantify the film and macropore resistances. The molecular diffusivity, D_m, and the Knudsen diffusivity, D_K, both contribute to the effective diffusivity, D_e, so that

$$\frac{1}{D_e} \propto \frac{1}{\tau'}\left[\frac{1}{D_m} + \frac{1}{D_K}\right] \tag{5}$$

in which the tortuosity factor, τ', is introduced to account for local macropore morphology. In the case of microporous materials such as zeolites, the main contribution to micropore diffusion comes from surface diffusion and, therefore, $D_c \approx D_s$. Since all contributions to the mass transfer resistance are lumped together into a single parameter, k^{ldf}, a simple expression for the transient behavior of the average adsorbate concentration in the particle, $\overline{q}(t)$, can be written as

$$\frac{\partial \overline{q}(t)}{\partial t} = k^{ldf}[q^* - \overline{q}(t)] \tag{6}$$

which can be solved simultaneously with transient mass balance equations that describe fixed-bed adsorber dynamics. The LDF approximation offers a practical alternative to estimate overall mass transfer in an adsorption process by conveniently avoiding the simultaneous detailed calculation of coupled mass transfer mechanisms that span different time scales. However, assuming that intracrystalline resistance is dominant in the adsorbent would yield the LDF coefficient:[70]

https://doi.org/10.1021/jacs.4c03086
J. Am. Chem. Soc. XXXX, XXX, XXX−XXX

$$k^{ldf} = \frac{15D_c}{r_c^2} \text{ and } \frac{D_c t}{r_c^2} = \frac{t}{\tau} > 0.1 \quad (7)$$

The time required for a given displacement of diffusing molecules is proportional to the square of the characteristic distance that needs to be traveled. By normalizing D to this distance, the diffusion coefficient can be described in units of time, referred to as τ, the diffusional time constant. The criterion given by eq 7, for which the LDF approximation holds, i.e., a long contact time t compared to the time constant τ, namely $\frac{t}{\tau} > 0.1$, corresponds to an equilibrium separation. Although successfully implemented for these processes, the LDF approach offers far less insights into the transport behavior at the adsorbent particle level compared to experimentally determined diffusion coefficients for the adsorbent crystals.[11,71] The LDF model assumes all adsorbate species diffusing independently of one another. However, the thermodynamic coupling between species needs to be considered to correctly describe the nonmonotonous approach to equilibrium in kinetic separations. The LDF model fails in adequately modeling this behavior, resulting in underestimated productivities for kinetic separations in fixed bed adsorbers. The Maxwell-Stefan diffusion equations, an extension of the Fick's diffusion equations that includes mutual interactions between adsorbates, have been shown to quantitatively describe transient uptake curves accurately.[72,73]

Measuring Transport Diffusion in Powders and Pellets. Despite the variety of available measurement methods, unraveling the intrinsic transport behavior of molecules in nanoporous materials (D_c in the previous section, further referred to as D), remains challenging. The techniques can be classified into microscopic, mesoscopic, and macroscopic based on the considered length scale. Microscopic techniques, including pulsed-field gradient NMR (PFG-NMR) and quasi-elastic neutron scattering (QENS), generally characterize the intracrystalline diffusion excluding potential surface barriers.[74] Computational approaches aim at describing the behavior at the microscopic scale as well, because of the time scales considered and the difficulties in describing crystal surfaces. Both PFG-NMR, QENS and simulations are limited to fast-diffusing adsorbate−adsorbent pairs ($D > 10^{-12}$ m^2/s) because of the limited time span and displacement that can be probed.[75] The limited preservation of the nuclear magnetization (PFG-NMR) and the profile of the scattering features (QENS) prohibit the characterization of movements that are too slow relative to the coverable time and distance.[76,77]

Mesoscopic methods such as interference (IFM) and infrared (IRM) microscopy allow direct monitoring of guest uptake profiles and diffusional fluxes in individual crystallites.[78] As a result, these methods enable assessing the effect of surface boundaries.[79,80] However, IFM and IRM require large crystals (>50 μm) due to the limited spatial resolution,[76,78] which is well beyond the crystal sizes used in practice (~1 μm). Because of the requirement for large crystals, these techniques can only be applied to relatively fast diffusing adsorbates. For example, for the combination of a 50 μm crystal and a guest molecule with a diffusion coefficient of 10^{-17} m^2/s (e.g., CO_2 in UTSA-16[81]), reaching equilibrium would take over two years (diffusion-limited uptake process for one-dimensional diffusion through a crystal).[75] Yet, diffusivity values estimated in larger crystals are not often directly transferable to smaller ones because of the impact on diffusion caused by crystal defects, surface barriers, etc.

In macroscopic techniques, the considered diffusion path vastly exceeds the dimensions of the individual crystallites.[76] Therefore, the diffusivity values obtained from these techniques are not estimated directly. Frequently used methods include volumetric or gravimetric uptake/release experiments,[82] the zero-length-column technique (ZLC),[83] frequency response methods (FR),[84] and dynamic column breakthrough experiments.[85]

The measurable diffusion coefficients D (m^2/s) as a function of the adsorbent particle size (μm) is indicated for several meso- and macroscopic methods in Figure 2. These techniques typically assess the transport diffusion of adsorbates, the mass transfer coefficient relevant to their industrial implementation. Microscopic techniques generally study (self-)diffusion at equilibrium rather than transport diffusion. Hence, they are only included to a minor extent since the focus of this perspective is on practical separations. All techniques presented in Figure 2 are subject to practical limitations, i.e., there is a limit on measuring fast gas-adsorbent pairs. These limitations stem from the blank response of the experimental setup itself, the time resolution of the equipment or the achievable perturbation frequency of the apparatus. The indicated boundaries for each technique are listed in Table S1 of the Supporting Information. The diagonal lines in Figure 2 correspond to the diffusional time constant τ (s), with $\frac{1}{\tau} = \frac{D}{r^2}$ with r (μm) as the radius of the crystal or pellet. This representation enables rapid visualization of the relation between the diffusion coefficients, the size of a crystal/pellet, and the diffusional time.

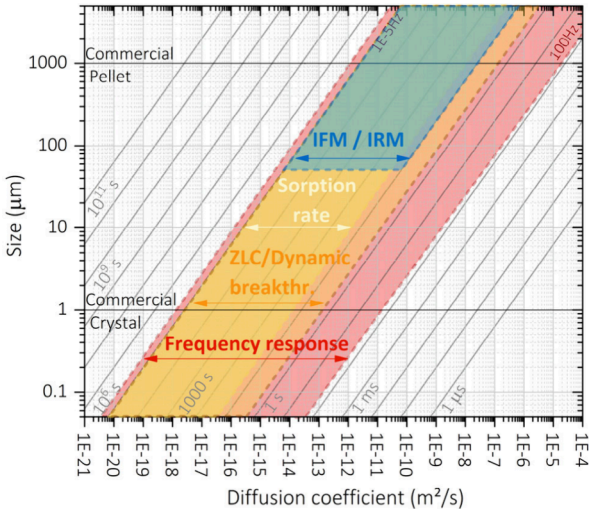

Figure 2. Window of experimentally determinable diffusivities D (m^2/s) for different techniques, sorption rate[82] (yellow), chromatographic methods (zero length column and dynamic breakthrough)[83,86] (orange), frequency response[84,87] (red), interference and infrared microscopy[75,88,89] (blue), in relation to the crystal/pellet size (μm). The diagonal lines refer to the diffusional time constants τ (s), with $\frac{1}{\tau} = \frac{D}{r^2}$. Conveniently used crystal (1 μm) and pellet (1 mm) sizes are marked with a horizontal line. A tabular form of the implemented boundary conditions per technique is presented in Table S1, Supporting Information.

https://doi.org/10.1021/jacs.4c03086
J. Am. Chem. Soc. XXXX, XXX, XXX−XXX

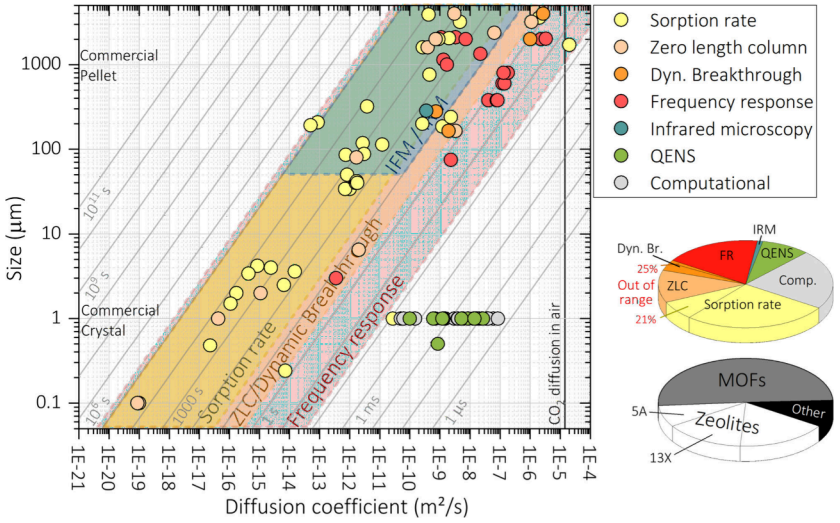

Figure 3. Values for experimental diffusion coefficients of CO_2 in a series of adsorbents, collected from the open literature, are plotted together with the reported size (μm) of the studied crystals/pellets and the measurement technique used. Colored areas represent the window of measurable diffusivities D (m^2/s) for different techniques in relation to the size of the crystals/pellet (μm). Typically used crystal and pellet sizes, and the bulk diffusion coefficient of CO_2 in air are marked. The diagonal lines refer to the diffusional time constants τ (s), with $\frac{1}{\tau} = \frac{D}{r^2}$. The fraction of entries per measurement technique is represented in the upper pie chart. The percentages indicate the fraction of entries outside of the acceptable range for the measurement technique that was used. Only dynamic breakthrough and sorption rate entries are found outside of the acceptable windows. The bottom pie chart represents the different classes of CO_2 adsorbents (zeolites (white), MOFs (gray) and other materials (black)). For zeolites, the fractions of the entries corresponding to 13X and 5A are marked separately.

For the most applied measurement technique, the sorption rate method, the measurable window of diffusivity values is rather limited: a range of less than 4 orders of magnitude can be examined for a given crystal or pellet size. Even when the dead volume of the measurement setup is minimized, the pressure cannot be changed instantly. Because of this non-negligible time constant of the measurement system and the need for sufficient data points acquired during the transient uptake, diffusional time constants faster than ~1 min are difficult to measure.[82] Hence, for crystal sizes typically found in commercial adsorbents (~1 μm or a bit larger), one cannot reliably determine diffusivity values faster than 10^{-14} m^2/s with this technique. However, in equilibrium-based separations, promising materials usually (have to) display higher diffusivity values, which can only be measured reliably for larger crystals with the sorption rate method. Therefore, it is far from trivial to screen fast-diffusing adsorbent-adsorptive pairs for relevant crystal sizes. The ZLC technique extends the measurable range of diffusivities by an order of magnitude (10^{-18} m^2/s–10^{-13} m^2/s) for relevant adsorbent particle sizes. Even when applying the frequency response method in which a periodic perturbance is applied at a frequency up to 100 Hz, the fastest diffusivity values that can be measured reliably for μm-sized crystals are on the order of 10^{-11} m^2/s.

Dynamic column breakthrough experiments have also been used to determine diffusivities. In this approach, a gas stream (single or multicomponent) is flowed through an adsorbent bed and the effluent concentrations are monitored until it "breaks through", i.e., is detected on the outlet side, mimicking the separation on a process scale.[85] However, these experiments only provide an indirect way to obtain or verify the apparent diffusivity. These measurements are generally performed on shaped adsorbent as the pressure drop in the system and the change in the outlet flow due to adsorption make the data analysis more complex for powders. Further, one needs to carefully eliminate or describe additional factors such as heat effects and mechanical dispersion. However, the method is extremely useful for process optimization as it gives a down-scaled, realistic representation of an adsorption-based process, taking into account the various diffusional resistances, process parameters and multicomponent effects.

Reported Diffusivity Values for CO_2 in Nanoporous Materials. Values for experimental diffusion coefficients of CO_2 in a series of adsorbents were collected from the open literature, classified by the reported measurement technique, and displayed in Figure 3. Powder and pellet data were included from over 50 articles, listed in Table S3 of the Supporting Information. A comprehensive selection of materials is represented, including mainly zeolites and MOFs, complemented by some silica- and carbon-based materials. A full list of the adsorbents is available in Table S2. A wide range of diffusivity values is observed for CO_2 in nanoporous crystals, from 10^{-17} to 10^{-9} m^2/s; and for pellets from 10^{-10} to 10^{-5} m^2/s. Most observations fall within the measurable ranges for the different techniques. Data points outside or at the edge of the accessible range should be handled with caution. Computational methods and QENS probe similar short time and length scales, independent of the crystal size. Hence, to include them in Figure 3, they are plotted for an arbitrary crystal size of 1 μm. These techniques probe higher diffusivities not measurable with macroscopic techniques and for common crystal sizes.

DISCREPANCY IN MASS TRANSFER RATES WITHIN GAS–ADSORBENT PAIRS

Assessing the Spread in Reported Diffusivities, for Different Sample Forms. When compiling the literature data on CO_2 diffusivities, a large spread in reported values is observed. Likely, this span can be partially explained by the dependency of the transport diffusion on specific experimental and sample conditions. Yet, reproducibly measuring mass

https://doi.org/10.1021/jacs.4c03086
J. Am. Chem. Soc. XXXX, XXX, XXX−XXX

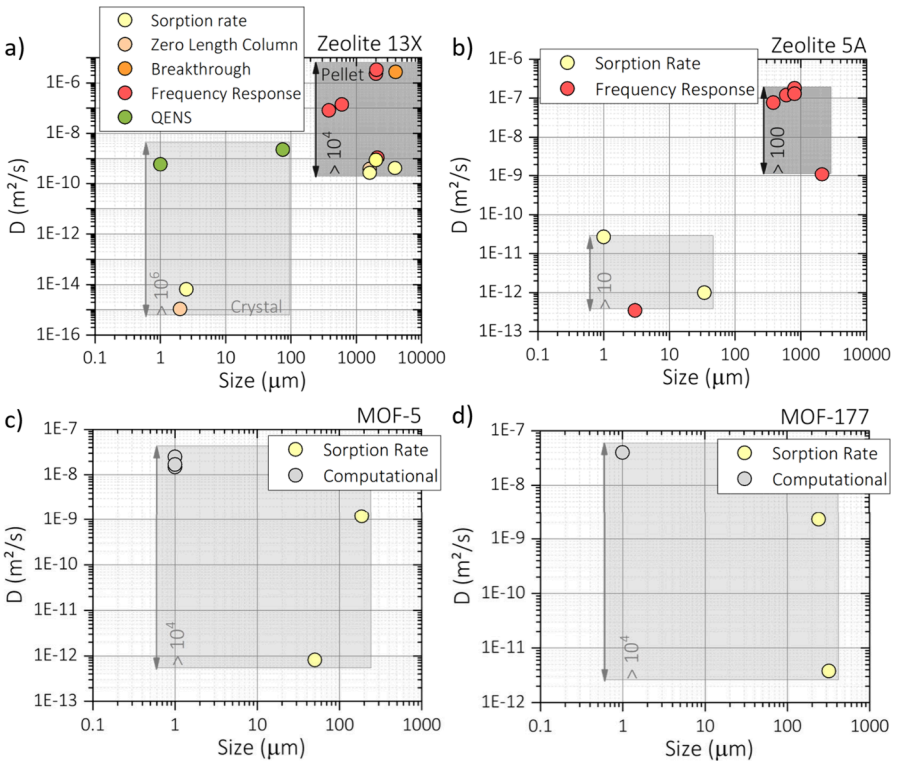

Figure 4. Diffusion coefficients (m^2/s) of CO_2 for different sizes of crystals (light gray area) and pellets (dark gray area) of (a) zeolite 13X and (b) zeolite 5A, colored per technique, and, for sorption rate and computationally obtained values for (c) MOF-5 and (d) MOF-177 on powder samples of MOF-177 (Figure 4c) and MOF-5 (Figure 4d).

transfer rates and reliably extracting diffusivity values is arguably harder than measuring and analyzing equilibrium data. Several factors can obscure the underlying adsorption rates or lead to erroneous diffusivities.

When comparing diffusion coefficients, one needs to evaluate whether the authors measured an equivalent mass transport process, i.e., self- vs transport diffusion, micropore diffusion vs (effective) macropore diffusion. And, hence, if the values are expected to correspond. Diffusion can be studied at different temperatures and loadings. These two factors impact the mass transfer process and can induce variability in the obtained diffusion coefficient values. The impact of these variables is strongly dependent on the adsorbate−adsorbent pair under study. As discussed earlier, different measurement methods probe different diffusional length scales. Significant differences in transport rates are reported when characterizing an adsorbate−adsorbent pair with micro- and macroscopic techniques. Moving from intracrystalline distances to a bed of crystals, additional factors, e.g., surface barriers and defects, come into play and strongly impact the observed adsorption rate. Different synthesis conditions also lead to variations in defect density and the presence or absence of surface barriers, impacting the observed rate of adsorption.[90−92] In addition, the defect density can change over time, depending on the stability of the adsorbent. Similarly, the contribution of surface barriers will become larger for smaller crystals.[93] Even crystals from the same synthesis batch, of similar size and shape, may show different rates of adsorption.[94]

Zeolites 13X and 5A have been widely studied for CO_2 capture applications, resulting in a relatively large number of publications on CO_2 mass transfer properties. Figure 4 depicts the diffusion coefficients measured for different sizes of crystals and pellets of zeolite 13X (Figure 4a) and 5A (Figure 4b). For both pellets and crystals, a large spread on the measured values is observed for 13X (>10 000× difference), and to a smaller extent for zeolite 5A (>100× difference). Likely, at least part of this spread is caused by measurements at different temperatures and loadings: several entries in the database report the temperature and loading dependency for 13X. Up to a difference approaching 1 order of magnitude is reported for a temperature change of 303 to 343 K, and up to a difference of 2 orders of magnitude for a CO_2 concentration ranging from 0.001 to 0.09 bar.[95,96] The inherent difference between micro- and macroscopic measurement techniques likely explains, to some extent, the spread between CO_2 diffusivities in 13X acquired by QENS and sorption rate experiments. Although fewer reports are available for specific MOF materials, multiple entries were compared. As for the zeolites, a large spread on the obtained diffusivities is also present for both CO_2-MOF couples (>1000× difference). Even for a single experimental approach (e.g., sorption rate), significant inconsistencies can be observed. Clearly, the diffusivity values derived from molecular simulations can be considered the upper limit. These calculations are often performed for an ideal framework, neglecting the presence of, e.g., defects, surface barriers, framework flexibility, and loading effects at higher concentrations (cf. the following section). In addition, the stability issues of some of these materials cannot be ignored and can result in differences between entries.

Still, it remains questionable whether the exposed discrepancies can be explained solely by different synthesis or measurement conditions. Unfortunately, inadequate execution of kinetic measurements is often raised as a significant concern and recognized as a major contributor to the spread in

https://doi.org/10.1021/jacs.4c03086
J. Am. Chem. Soc. XXXX, XXX, XXX−XXX

reported data.[48,97] An in-depth understanding of the experimental setup and its limitations are required to assess mass transport. Alongside rigorous sample prerequisites (e.g., uniform crystal size, fine sample dispersion, etc.) it is crucial to thoroughly evaluate the constraints of the experimental setup, choose an appropriate mathematical model, and ensure that the experimental design adheres to the model restrictions. Multiple experiments on different samples are needed to confirm the kinetic regime and the nature of the observed mass transfer phenomenon to exclude any impact of the experimental setup. Model assumptions need to be respected, yet commonly they are considered trivial, which is often far from true. In addition, the characteristic diffusion length needs to be precisely determined to extract the diffusivity using a model. Crystals or pellets of nonuniform particle size will result in an over- or underestimation of the intrinsic mass transfer behavior. When performing diffusivity measurements, a broad particle size distribution or irregularly intergrown crystals and aggregates are hard to quantify and often ignored.

Each method is bound to a series of verifications needed to confirm the observed underlying mechanism. Additional external factors that can impact or even dominate the overall observed mass transfer characteristics come into play as well, e.g., bed diffusion effects and heat dissipation. One needs to prove that these factors are insignificant or explicitly take these into account.[97,98] For the reported values in Figure 3, no assessment was made on the accuracy of the entries. Many of the reports might be observing a phenomenon different from what was anticipated. Erroneous assumptions and interpretations of the obtained data lead to unreliable results. Given the many parameters that impact the experimental outcome, comprehensively reporting all relevant specifications of the sample and experiment is needed to compare observations thoroughly. The IUPAC project on diffusion in nanoporous solids drives the awareness of obtaining and interpreting reliable experimental results via, among other initiatives, the reported comprehensive set of guidelines for measuring and reporting diffusion properties.[97]

COMPLEMENTARITY AND LIMITATIONS OF MOLECULAR SIMULATIONS

Molecular simulations have been instrumental in investigating diffusion in porous solids, providing mechanistic insights that are either challenging or impossible to obtain experimentally. The predominant techniques are based on molecular dynamics (MD), in which molecular trajectories are simulated, typically over tens or hundreds of ns, by integrating Newton's equation of motion from forces acting on individual atoms.[99] From the resulting trajectories, diffusion coefficients can be determined via the mean square displacement technique, the Green−Kubo expression, or from nonequilibrium methods.[100] As for experimental techniques, the range of diffusion coefficients that can be determined via MD is limited. Diffusivities smaller than 10^{-11}−10^{-12} m^2/s become intractable due to the limited displacement on the achievable observational time scale. Nevertheless, the accessible diffusivity range can be extended via techniques such as the transition state theory, in which diffusion is described by a hopping probability between two adsorption sites.[101]

In many cases, diffusivities determined through computational methods are several orders of magnitude faster than experimentally macroscopically determined values for the same adsorptive-adsorbent pair. These discrepancies stem mainly from differences in probed time scales (and, thus, length scales) and how representative the crystal lattice models are. While most experimental methods probe longer time and length scales, a direct comparison with computational results is, in theory, possible using PFG-NMR (for large crystals) or QENS data. However, even when comparing with these experimental methods, the discrepancy between the ideal crystal lattice assumed in computational methods and the nonideal nature of the sample (e.g., due to the presence of defects) can lead to different diffusivity values.[102] These differences can become very large for macroscopic experimental techniques due to the additional surface barrier resistances that cannot be accounted for in simulations as the molecular structure of the crystal surface is ill-defined. Another obstacle are the errors in many reported crystal structures,[103] which may affect the calculated diffusivities and limits the leverage computational methods can offer through database screening. Moreover, the choice of force field and whether or not framework flexibility is taken into account can have a significant impact on the resulting diffusion coefficients.[104−107]

Nevertheless, for largely defect-free zeolite crystals synthesized using the fluoride method, relatively good agreements have been reported between molecular simulations,[108] PFG-NMR,[109] microimaging[110] and macroscopic techniques (Zero Length Column,[111] frequency response[46]). In other cases, MD simulations have provided valuable insights into intracrystalline diffusion mechanisms.[112−114] While for many zeolites the self-diffusivity decreases monotonically with loading,[115,116] non-monotonic behavior has been observed for zeolites consisting of cages separated by narrow windows or in the presence of cations. For example, in Na-ZSM-5, the strong interaction of CO_2 with the sodium sites results in low diffusivities at low loadings. At higher loadings, when the cation sites are saturated, the diffusivity increases before finally decreasing again due to pore saturation.[117]

Molecular simulations are also a powerful tool for studying multicomponent diffusion, for which experimental data is rarely reported because of shortcomings of current measurement techniques. For instance, by combining MD simulations and QENS data on CO_2/CH_4 mixture diffusion in UiO-66, it was found that as the CO_2 loading increases, the CH_4 diffusivity initially rises and then falls.[118] By analyzing the MD trajectories, it was shown that the preference of CO_2 for the tetrahedral cages pushes CH_4 into the octahedral ones, in which weaker interactions with the pore wall occur, reducing the energy barrier for CH_4 hopping and enhancing its diffusivity. This enhancement in the diffusion rate due to the presence of another guest molecule contrasts with predictions for narrow-pore zeolites, in which the molecules are expected to diffuse independently[119,120] (i.e., having no influence on each other) or in which the faster diffusing CO_2 hinders the diffusion of the slower diffusing CH_4.[121] For an exhaustive list of insights derived from MD simulations, the reader is directed to excellent reviews on the subject.[102,122−124] Since the limitations indicated above evidently hold for multicomponent diffusion, simulation outcomes should be viewed as a realistic representation only for near-ideal crystal domains, and even then, diffusivity differences are likely more meaningful than absolute values to understand the underlying mechanisms and help guide the design of new adsorbents with targeted diffusion properties, for both equilibrium and kinetic separations.

https://doi.org/10.1021/jacs.4c03086
J. Am. Chem. Soc. XXXX, XXX, XXX−XXX

Molecular simulations also face challenges in capturing both nanopores and wider channels in hierarchically structured materials due to the large difference in length scales. However, as computational resources evolve and interconnected pore networks can be mapped better through high-resolution tomography, multiscale simulations will improve to help understand these complex systems.[125−127] For instance, recently, MD techniques were developed to simultaneously study the temperature dependence of intra- and intercrystalline diffusion of *n*-hexane in zeolite NaY.[128] At lower temperatures (200 K), strong adsorption restricts the movement of the molecules within the crystal and desorption into the intercrystalline space where fast diffusion can occur. Conversely, at higher temperatures (800 K), the higher concentration of molecules in the intercrystalline region results in a much higher overall diffusivity.

DOMINATING MICRO- VS MACROPORE MASS TRANSFER RESISTANCE

In an adsorption process, molecules subsequently diffuse through the large pores in the pellet and the micropores in the adsorbent. Evidently, the diffusivity in the interparticle space in the pellet is typically (much) higher than in the crystals. However, because of the much larger size of the pellet compared to the adsorbent particles (typically mm vs μm), the overall time constant of the adsorption process can be dominated by either diffusion stage. This process time constant determines the cycle time and, therefore, the productivity that can be achieved.

In equilibrium separations, mass transfer ideally occurs at the high rate allowed by macropore diffusion (i.e., micropore diffusion is not limiting). In that scenario, equilibrium is reached faster for smaller pellets. However, the pressure drop over the bed constrains the minimum pellet size,[40,129,130] especially in rapid PSA processes, which operate at high gas velocity. Decreasing the pellet size by an order of magnitude will increase the pressure drop over the bed by approximately 2 orders of magnitude.[20] Two examples of process intensification efforts aimed at enhancing mass transfer while overcoming an increased pressure drop are the development of structured adsorbents (such as monoliths, coated fibers or sponges),[129−132] and the introduction of macro/mesopores into a microporous material to realize "hierarchically structured" adsorbents.[133,134] However, while structures such as monoliths enable operation at higher gas velocities and shorter cycle times compared to conventional adsorbers packed with pellets, they still present a trade-off between adsorption capacity and mass transfer: the latter is improved at the cost of a lower bed capacity. Therefore, such structured adsorbents are especially interesting in the case of trace removal, where high capacity is less important than high affinity. An example is Direct Air Capture (DAC), discussed below. In contrast, in kinetic separations, the process time constant is necessarily determined by the intrinsic kinetics of the microporous crystals to achieve selectivity.

When performing kinetic experiments on pellets, usually via macroscopic techniques, a diffusivity value is extracted by fitting a suitable model (e.g., for diffusion in a spherical particle). In doing so, the pellet is considered a homogeneous medium, leading to an effective diffusivity in which all underlying mass transfer resistances are lumped together. In the absence of micropore diffusion limitation, these values are expected to be much larger than the inherent diffusivities of the adsorbent crystals. As can be seen in Figures 4a and 4b for zeolites 13X and 5A, respectively, this is indeed the case for most reported values. However, in that data set, the powder and pellet entries were obtained from independent studies, meaning that the crystals used were not identical (e.g., because of different synthesis conditions).

In diffusivity measurements on pellets, the dominating resistance (micro- vs macropores) can be determined by varying the experimental conditions (e.g., crystal and pellet sizes, carrier gas and flow rates, etc.), or, although far less recommended, from fitting model parameters. Figure 5 shows

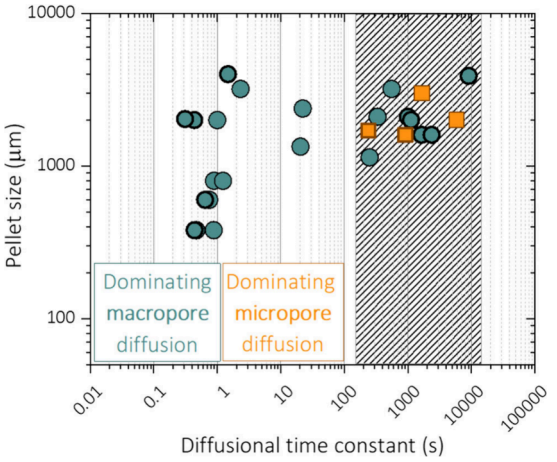

Figure 5. Diffusional time constants τ (s) of CO_2 in pellets of different adsorbent materials for studies indicating the dominating diffusivity, macropore-controlled (blue circles) or micropore-controlled (orange squares). The dashed area illustrates the time domain where both controlling mechanisms overlap. The symbols corresponding to zeolite 13X are highlighted by an increased edge line width.

measured diffusivities for pellets for studies in which the dominating resistance was determined by these approaches. In only four cases, micropore diffusion was found to be dominating. Nevertheless, at longer diffusional time constants (approximately 10^2−10^4 s, gray area), pellets in which micro- and macropore diffusion reportedly dominate appear together, even for pellets consisting of similar binders and crystals (e.g., zeolite 13X, highlighted in Figure 5). In other words, when considering these results together, it is not evident that micropore diffusion indeed plays a negligible role in the overall mass transfer. It is necessary to experimentally deduce the underlying mechanism of the observed behavior to conclusively assign the dominating resistances in a shaped adsorbent.

An independent measurement of the mass transfer rate in the primary adsorbent particles (in powder form) would indicate the role of the intrinsic mass transfer rate when incorporated in a shaped adsorbent. Unfortunately, only one study in the compiled database reports diffusivity measurements on the same zeolite crystals in powder and pellet form.[135] Nevertheless, such studies provide valuable information and can flag issues such as the intrusion of heat transfer limitations in pellet measurements. Since adsorption is an exothermic process, and the guest uptake is lower at higher temperatures, care must be taken to remove the released heat of adsorption sufficiently rapidly to avoid heating up the adsorbent. If this is not the case, the guest uptake kinetics

https://doi.org/10.1021/jacs.4c03086
J. Am. Chem. Soc. XXXX, XXX, XXX−XXX

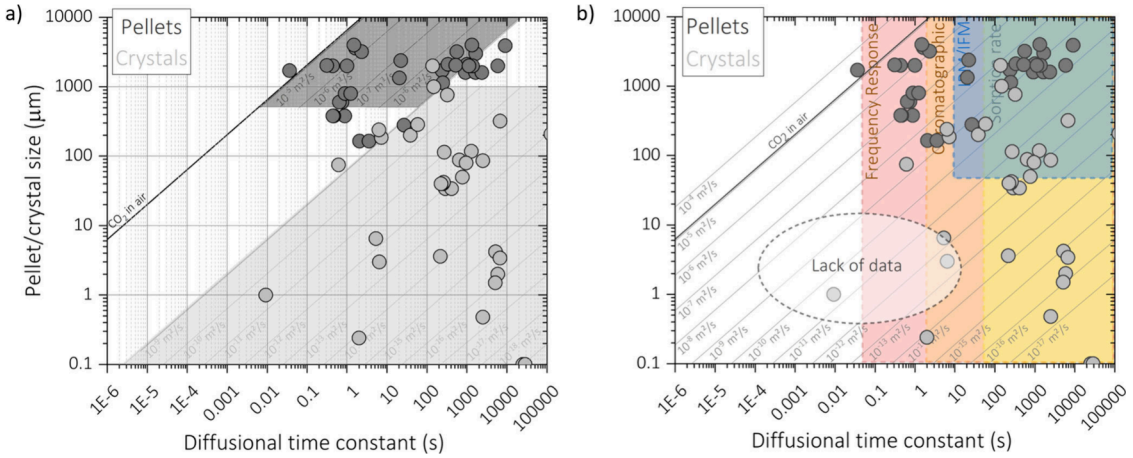

Figure 6. Diffusional time constants of CO_2 in powders (light gray circles) and pellets (dark gray circles) plotted against the pellet or crystal size. The diagonal lines present the respective diffusion coefficients (m^2/s); the line corresponding to the bulk diffusion coefficient of CO_2 in air is highlighted. The shaded areas represent (a) the range of time constants for crystals (light gray) and pellets (dark gray) calculated from measured diffusivity ranges and characteristic diffusion lengths, and, (b) the accessible time constant ranges of several experimental techniques. The white-shaded area with dashed outline in panel b highlights the lack of data for small diffusional time constants.

might be limited by the cooling rate of the adsorbent, even if the intrinsic mass transfer is much faster (i.e., rapidly reaching equilibrium at each adsorbent temperature). In measurements on powder samples, isothermal conditions can more easily be guaranteed, e.g., by dispersing a small amount of sample in a thin layer on a thermally conducting substrate. For pellets (and especially beds thereof), it is far less trivial to remove the heat of adsorption sufficiently rapidly, and errors in the extracted diffusivity values are readily introduced, even for small temperature changes.[136] It is therefore not unlikely that some of the pellet entries in Figures 4 and 5 are questionable.

Since the mechanisms governing macropore diffusion are largely material-independent, diffusivities generally fall in the relatively narrow range of 10^{-5} to 10^{-9} m^2/s, depending on the relative size of the adsorbates and the adsorbent pore, and, several shaping-related parameters (porosity, tortuosity, etc.).[137,138] Micropore diffusivities span a much wider range at lower values, from 10^{-9} to 10^{-18} m^2/s or even slower.[139] Figure 6a illustrates the span of time constants for crystals (light gray area) and pellets (dark gray area) when combining these diffusivity ranges with typical sizes (roughly from 1 μm to 1 mm for crystals vs >0.5 mm for pellets, respectively). The resulting time constant range for pellets lies within the range for crystals. In other words, it is far from trivial to assume that micropore diffusion will not be limiting, and the intrinsic diffusion behavior of the adsorbent crystals might determine the overall process time constant. The same conclusion is also reached by plotting all reported diffusional time constants for both powders (including some amorphous carbon and silica materials) and pellets in the compiled literature database (Figure 6a): the relatively large time constants associated with some microporous crystal entries indicate that these adsorbent materials would be the limiting factor in the CO_2 mass transfer when shaped into pellets, even for crystal sizes of 1 μm or below. This observation indicates that the intrinsic CO_2 diffusivity of a microporous adsorbent should be considered as an additional criterion when targeting equilibrium-based CO_2 separations, next to high selectivity and uptake capacity. Thus, far, this aspect has been a blind spot and adsorbents have been mostly suggested based on isotherms (i.e., equilibrium data).

Based on the crystal and pellet entries in Figure 6, it even appears hard to select an adsorbent material for which micropore diffusion would not become limiting: for most crystal entries, the time constant is comparable to or even larger than for pellets. However, this apparent contradiction with the earlier statement that pellet measurements often indicate dominating macropore diffusion (see Figure 5) is at least partly explained by the limitations of the available experimental techniques (Figure 6b). The region of the graph where adsorbents with fast intrinsic CO_2 diffusion would be expected to appear, shaded in white, is currently experimentally nearly inaccessible because of time constants well below 1 s for relevant crystal sizes (1 to 10 μm). The entry that appears in this region is clearly outside of the measurable range and should be approached cautiously. On the other hand, based on the collected data, a rough selection guideline can be formulated for adsorbent materials suitable for equilibrium separations based on the minimum required CO_2 diffusivity. Considering an average diffusion coefficient of 10^{-7} m^2/s for 1 mm pellets results in $\tau_{macro} \approx 2.5$ s. When $\frac{\tau_{macro}}{\tau_{micro}} > 10$, the intrinsic kinetic behavior of the adsorbent material is significantly faster than the mass transport through the pellet and could be considered negligible to the overall process time constant. Therefore, with this criterion, τ_{micro} should be lower than 0.25 s, which translates to a micropore diffusivity greater than 10^{-12} or 10^{-10} m^2/s for reasonable crystal sizes of 1 to 10 μm, respectively (see Figure 6). If the intrinsic diffusivity in the crystals is slower than these values, decreasing τ_{micro} by preparing smaller crystallites is, in principle, possible. However, shaping adsorbent pellets from crystals much smaller than 1 μm would be far from trivial (e.g., maintaining macropores when using a binder with a similarly small particle size). Conversely, such materials with slower intrinsic CO_2 diffusivities can be of great interest for kinetic separations or membrane separations. When the CO_2 diffusivity is low compared to the diffusivities of the other adsorbates present, a kinetic separation with a high purity CO_2 outlet can be established.

https://doi.org/10.1021/jacs.4c03086
J. Am. Chem. Soc. XXXX, XXX, XXX−XXX

ADDITIONAL CONSIDERATIONS FOR CO_2 CAPTURE

Presence of Water in the Gas Stream. As water is unavoidable in most carbon capture scenarios, understanding its impact on CO_2 adsorption and diffusion is critical. A fair amount of literature exists on multicomponent CO_2/H_2O adsorption,[140] showing a wide variety of behaviors, with materials where CO_2 uptakes are barely influenced by the presence of water to completely suppressed adsorption.[141] Some studies have even shown an enhancement in CO_2 uptake under specific conditions[142−144] where water serves as an additional CO_2 adsorption site. Despite these efforts, the difficulty of performing these equilibrium measurements has recently been highlighted,[145] together with the need for new, less time-consuming techniques to enable more systematic studies.

Regarding the influence of water on CO_2 diffusion, the literature is scarce, as emphasized in a recent review.[146] Apart from a few simulation studies, only one QENS study reported experimental results on the impact of the hydration level on the CO_2 mobility in clay materials.[147] Nevertheless, these works highlighted some interesting behaviors. In CO_2-H_2O multicomponent simulations, more water molecules adsorbed into the pores of the MOFs UiO-66 and CALF-20 gradually reduced the CO_2 diffusion coefficients.[114,148] In MOFs with open metal sites (OMS), such as MOF-74, a segregation between the stronger adsorbing water molecules and CO_2 has been shown due to the stronger adsorption of the former close to the OMS, which in turn leads the latter to move more freely.[149] Another study on ternary mixtures of CO_2, N_2, and H_2O showed that in IRMOF-1 the mobilities of these molecules are similar in single- and multicomponent scenarios, while the diffusivities of CO_2 and water in Cu-BTC were reduced in the ternary mixture. The opposite behavior is observed in MIL-47, where the adsorbate species diffuse faster in the mixture than they do as pure components.[150]

These computational studies highlight the diverse behavior of CO_2 diffusion in the presence of water. Due to the complexity of experimentally measuring multicomponent diffusion, it has not yet been possible to validate these findings, nor to investigate the impact of defects, other diffusional resistances, or shaping. This knowledge gap calls for an increased effort to understand the impact of water on CO_2 diffusion as the impact on the overall productivity of a carbon capture process might be significant.

Chemisorbents for CO_2 Capture. So far in this Perspective, only materials that adsorb CO_2 via physisorption have been discussed. On the other hand, amine-functionalized sorbents react with CO_2 through a chemisorption mechanism similar to CO_2 capture by aqueous amine solutions.[151] By fixing amines in porous solids such as mesoporous silica,[152,153] polymers,[154] carbons,[155] and MOFs,[156] the energy required to regenerate the adsorbent is lowered significantly compared to aqueous amine scrubbers.

Due to the high affinity of the amine groups for CO_2, chemisorbents can be highly selective for CO_2 even in the presence of water. Under dry conditions, the favored reaction mechanism seems to be forming an ammonium carbamate with a 1:2 CO_2:amine stoichiometry. In the presence of water, forming ammonium bicarbonate or hydronium carbamate species is favored, where the stoichiometry is 1:1. This difference in stoichiometry in dry and wet conditions is at the origin of the enhanced CO_2 capacity in the presence of water.[157−162] However, this simplified picture might be incomplete as there are often likely multiple mechanisms in play, as exemplified by the dependence of the humidity-driven CO_2 uptake enhancement on the CO_2 pressure, humidity, and temperature in Lewatits VP OC 1065, an amine-functionalized cross-linked polymer.[163] Diamine-appended MOFs also show an unusual cooperative insertion mechanism[164] where the metal-bound amine group reacts with CO_2 to generate a carbamate while the pendent amine is protonated. This process propagates through the material to yield ammonium carbamate chains stabilized through ionic interactions. As a result of this mechanism, these materials exhibit step-shaped CO_2 adsorption profiles, which give rise to large CO_2 cycling capacities that are accessible via relatively small temperature or pressure swings.

In contrast to physisorbents, where the mass transfer is determined by the diffusion of guest molecules in the porous framework, the reaction kinetics between the amine groups and CO_2 can dominate uptake rates for chemisorbents. Amine-functionalized materials can be categorized into (i) materials in which the pores have been impregnated with liquid amines, (ii) micro- or mesoporous materials with amine functionalities grafted on their inner pore surface, and (iii) macroporous amine-functionalized polymers. In the first category, slow intrapore liquid phase diffusion is to be expected. In the second category, depending on the pore and crystal sizes, a combination of intracrystalline diffusion and reaction kinetics affects the uptake rate. Well-known commercial materials in the third category are Purolite and Lewatit, which are obtained as microporous spheres with a size between 300 and 1250 μm via copolymerization. Therefore, intraparticle diffusion is expected to be fast, and the reaction kinetics are likely rate-limiting.

Attempts have been made to study kinetics in amine-functionalized materials via experiments and modeling. For example, a ZLC study identified distinct mass transfer regimes (surface diffusion followed by diffusion from the polymer chains). Gravimetric uptake experiments on polyethylenimine-functionalized materials indicated the need for higher-order kinetic laws to describe the uptake mechanism.[165] Other studies found that the uptake kinetics can be well described using a kinetic model based on the reaction mechanisms of CO_2 in supported amines in dry and humid conditions and a simple linear driving force model to transport. While it thus appears that, in many cases, the reaction of CO_2 is the rate-limiting step in DAC materials, the contribution of diffusion and reaction kinetics in the overall rate has not yet been disentangled. A multidisciplinary approach will be needed, combining macroscopic and microscopic measurements with modeling to extract the intrinsic, fundamental parameters. Understanding the CO_2 adsorption kinetics in these materials, particularly in the presence of water, is critical for their evaluation as this property will ultimately dictate the achievable productivity.

CONCLUSION AND OUTLOOK: BRIDGING MASS TRANSFER EXPERIMENTS AND INDUSTRIAL APPLICATIONS

Evaluating an adsorbent based on equilibrium data (i.e., capacity and selectivity) alone does not provide the full picture needed to assess its separation potential. While knowledge of mass transfer is required to fully understand and optimize a

https://doi.org/10.1021/jacs.4c03086
J. Am. Chem. Soc. XXXX, XXX, XXX−XXX

separation process, the complexity of diffusion phenomena over multiple length scales and the limitations of both computational and experimental techniques remain challenging. For instance, measuring fast diffusion ($>10^{-11}$ m^2/s) is currently not possible for practically relevant crystal sizes (~1 μm). Even for a separation as significant as CO_2 capture, only few experimental mass transfer studies are available. As highlighted by IUPAC, the scarcity and inconsistencies in mass transfer studies on nanoporous materials result in a partial understanding of these processes in technological applications.[97]

On the other hand, it could be questioned if such measurements are necessary for equilibrium separations since, for practical purposes, it may suffice to determine whether or not a candidate adsorbent meets a threshold, such as the 10^{-12} m^2/s criterion proposed above for 1 μm crystals. However, even then, only the extended, hence, unconventional regime of the frequency response method (applied frequency >10 Hz) enables measuring such a short time constant. Other techniques, such as the sorption rate and chromatographic methods, can only measure diffusivity values for crystals approximately 10 times larger than the relevant size range. When feasible, large crystals require different synthesis conditions compared to industrially relevant materials and might not be fully representative since differences in synthesis protocols are known to affect mass transfer rates. Because of these reasons, novel measurement methods that enable access to the fast-diffusion regime for relevant crystal sizes are needed to unambiguously select promising materials.

Kinetic separations are a promising route for cases where equilibrium selectivities provide unsatisfactory results due to the (potentially) larger differences in kinetic selectivity. Even for similar molecules, intracrystalline diffusivities can be orders of magnitude apart. Although modeling and evaluating kinetic separations are more complex because of the need to consider multicomponent diffusion, the number of reports in this area is increasing. It has been shown that LDF models drastically underestimate the productivity achievable in kinetic separations as thermodynamic coupling effects are not considered. Improvements have been made to couple lab-scale parameters to large-scale applications, exposing the crucial role of crystal size and contact time in fixed bed adsorbers to optimize productivity.[11] Effectively, this relation underlines the fine line between equilibrium and kinetic separations for a given adsorbent-adsorptive pair. The intricate interplay between multicomponent equilibria, mass transfer rates, crystal size, and contact time can drive the process in a certain direction, from equilibrium to kinetically controlled operation. Yet, more data and refined process models are needed to fully exploit the potential of kinetic separations and extend their adoption at industrial scales.

Throughout this Perspective, the focus has been on experimentally obtained single-component diffusion data. However, in industrial applications, competing adsorbing species will affect the findings from single-component measurement data, at the micropore level but potentially also for macropores, e.g., by altering diffusion from the bulk to the particle surface.[166] Water and impurities in gas streams can also impact adsorbent stability, uptake capacity, and mass transfer rates.[167] Reliable experimental data is scarce for competitive equilibria of multicomponent systems[166] and even more so for multicomponent diffusion measurements.[84] This is unsurprising since the experimental effort increases dramatically for multiple adsorbates, and the techniques require specialized equipment and know-how.[168] This will most likely change as new measuring techniques and computational methods continue to develop.

Given the various interactions and mechanisms at play, predicting mass transfer rates in powders and shaped adsorbents remains challenging. For every separation process, selecting an optimal adsorbent−process couple starts with experimentally determining the mass transfer at the crystal level, supported by mechanistic insights from molecular simulations. To optimize the shaped form and its performance in a bed, the critical translation from the crystals into a shaped entity should be studied in more detail, i.e., measuring the primary adsorbent particles as such and in their shaped form. These accurate values are needed for the reliable design of practical adsorption processes using multicomponent process models. In addition, this information can serve the further development of multiscale numerical schemes. Multicomponent breakthrough experiments can help to establish adsorbent productivity by linking together the lab and process scales and revealing their interdependencies. Robust experimental data on mass transfer properties during both the material design and shaping stages, coupled with the advancement of sophisticated models to accurately describe multicomponent scenarios, are essential to address the remaining gaps and fully harness the potential of integrating nanoporous materials in separation processes.

■ ASSOCIATED CONTENT

Supporting Information

The Supporting Information is available free of charge at https://pubs.acs.org/doi/10.1021/jacs.4c03086.

Boundary conditions of experimental methods and compiled literature database (adsorbents, year, diffusion coefficient, reference) (PDF)

■ AUTHOR INFORMATION

Corresponding Authors

Nicolas Chanut − *Center for Membrane Separations, Adsorption, Catalysis and Spectroscopy (cMACS), KU Leuven, 3001 Leuven, Belgium*; Email: nicolas.chanut@kuleuven.be

Rob Ameloot − *Center for Membrane Separations, Adsorption, Catalysis and Spectroscopy (cMACS), KU Leuven, 3001 Leuven, Belgium*; orcid.org/0000-0003-3178-5480; Email: rob.ameloot@kuleuven.be

Authors

Margot F. K. Verstreken − *Center for Membrane Separations, Adsorption, Catalysis and Spectroscopy (cMACS), KU Leuven, 3001 Leuven, Belgium*

Yann Magnin − *TotalEnergies, OneTech, R&D, CSTJF, Pau 64800, France*; orcid.org/0000-0002-4603-632X

Héctor Octavio Rubiera Landa − *Department of Chemical Engineering & Industrial Chemistry, Vrije Universiteit Brussel, B-1050 Brussels, Belgium*

Joeri F. M. Denayer − *Department of Chemical Engineering & Industrial Chemistry, Vrije Universiteit Brussel, B-1050 Brussels, Belgium*; orcid.org/0000-0001-5587-5136

Gino V. Baron − *Department of Chemical Engineering & Industrial Chemistry, Vrije Universiteit Brussel, B-1050 Brussels, Belgium*

https://doi.org/10.1021/jacs.4c03086
J. Am. Chem. Soc. XXXX, XXX, XXX−XXX

Complete contact information is available at:
https://pubs.acs.org/10.1021/jacs.4c03086

Notes

The authors declare no competing financial interest.

■ ACKNOWLEDGMENTS

The authors acknowledge the KU Leuven for funding in research project C14/20/085. M.F.K.V. and N.C. acknowledge the Research Foundation Flanders (FWO Vlaanderen) for an SB doctoral fellowship (1S48221N), and a junior research project (G0A1B24N). This project has received funding from the European Research Council (ERC) under the European Union's Horizon Europe research and innovation programme (grant agreement no. 101045433, acronym: KISSIES). H.O.R.L. would like to acknowledge the support of Agentschap Innoveren & Ondernemen (VLAIO) of the Government of Flanders, Belgium, through Moonrise-MOONSHOT Project HBC.2020.2612 (3E210291): "Hybrid membrane/sorption technology for more efficient C2 and C3 separations."

■ ABBREVIATIONS

PSA, pressure swing adsorption; TSA, temperature swing adsorption; CMS, carbon molecular sieve; MOF, metal−organic framework; LDF, linear driving force; PFG-NMR, pulse field gradient nuclear magnetic resonance; QENS, quasi-elastic neutron scattering; IFM, interference microscopy; IRM, infrared microscopy; ZLC, zero length column; FR, frequency response; MD, molecular dynamics; OMS, open metal site

■ REFERENCES

(1) Sholl, D. S.; Lively, R. P. Seven Chemical Separations to Change the World. *Nature* **2016**, *532* (7600), 435−437.
(2) *Shell Scenarios | Shell Global*. https://www.shell.com/energy-and-innovation/the-energy-future/scenarios.html (accessed 2024-02-13).
(3) Paltsev, S.; Sokolov, A.; Gao, X.; Haigh, M. Meeting the Goals of the Paris Agreement: Temperature Implications of the Shell Sky Scenario. *In World Scientific Encyclopedia of Climate Change; World Scientific* **2021**, *1*, 333−339.
(4) D'Alessandro, D. M.; Smit, B.; Long, J. R. Carbon Dioxide Capture: Prospects for New Materials. *Angew. Chem., Int. Ed.* **2010**, *49* (35), 6058−6082.
(5) Choi, S.; Drese, J. H.; Jones, C. W. Adsorbent Materials for Carbon Dioxide Capture from Large Anthropogenic Point Sources. *ChemSusChem* **2009**, *2* (9), 796−854.
(6) Bui, M.; Adjiman, C. S.; Bardow, A.; Anthony, E. J.; Boston, A.; Brown, S.; Fennell, P. S.; Fuss, S.; Galindo, A.; Hackett, L. A.; Hallett, J. P.; Herzog, H. J.; Jackson, G.; Kemper, J.; Krevor, S.; Maitland, G. C.; Matuszewski, M.; Metcalfe, I. S.; Petit, C.; Puxty, G.; Reimer, J.; Reiner, D. M.; Rubin, E. S.; Scott, S. A.; Shah, N.; Smit, B.; Trusler, J. P. M.; Webley, P.; Wilcox, J.; Mac Dowell, N. Carbon Capture and Storage (CCS): The Way Forward. *Energy Environ. Sci.* **2018**, *11* (5), 1062−1176.
(7) Tian, Y.-J.; Deng, C.; Peng, Y.-L.; Zhang, X.; Zhang, Z.; Zaworotko, M. J. State of the Art, Challenges and Prospects in Metal−Organic Frameworks for the Separation of Binary Propylene/Propane Mixtures. *Coordination Chemistry Reviews* **2024**, *506*, 215697.
(8) Van Miltenburg, A.; Zhu, W.; Kapteijn, F.; Moulijn, J. A. Adsorptive Separation of Light Olefin/Paraffin Mixtures. *Chem. Eng. Res. Des.* **2006**, *84* (5), 350−354.
(9) Cui, W.-G.; Hu, T.-L.; Bu, X.-H. Metal−Organic Framework Materials for the Separation and Purification of Light Hydrocarbons. *Adv. Mater.* **2020**, *32* (3), 1806445.
(10) Wang, Y.; Peh, S. B.; Zhao, D. Alternatives to Cryogenic Distillation: Advanced Porous Materials in Adsorptive Light Olefin/Paraffin Separations. *Small* **2019**, *15* (25), 1900058.
(11) Krishna, R. Fundamental Insights into Intracrystalline Diffusional Influences on Mixture Separations in Fixed Bed Adsorbers. *Chem. Bio Eng.* **2024**, *1* (1), 53−66.
(12) Rouquerol, J. Recommendations for the characterization of porous solids (technical report). *Pure Appl. Chem.* **1994**, *66*, 1739−1758.
(13) Eum, K.; Jayachandrababu, K. C.; Rashidi, F.; Zhang, K.; Leisen, J.; Graham, S.; Lively, R. P.; Chance, R. R.; Sholl, D. S.; Jones, C. W.; Nair, S. Highly Tunable Molecular Sieving and Adsorption Properties of Mixed-Linker Zeolitic Imidazolate Frameworks. *J. Am. Chem. Soc.* **2015**, *137* (12), 4191−4197.
(14) Bhadra, S. J.; Farooq, S. Separation of Methane−Nitrogen Mixture by Pressure Swing Adsorption for Natural Gas Upgrading. *Ind. Eng. Chem. Res.* **2011**, *50* (24), 14030−14045.
(15) SIRCAR, S.; GOLDEN, T. C. Purification of Hydrogen by Pressure Swing Adsorption. *Sep. Sci. Technol.* **2000**, *35* (5), 667−687.
(16) Ritter, J. A.; Ebner, A. D. State-of-the-Art Adsorption and Membrane Separation Processes for Hydrogen Production in the Chemical and Petrochemical Industries. *Sep. Sci. Technol.* **2007**, *42* (6), 1123−1193.
(17) Yang, S.-I.; Choi, D.-Y.; Jang, S.-C.; Kim, S.-H.; Choi, D.-K. Hydrogen Separation by Multi-Bed Pressure Swing Adsorption of Synthesis Gas. *Adsorption* **2008**, *14* (4), 583−590.
(18) Farmahini, A. H.; Krishnamurthy, S.; Friedrich, D.; Brandani, S.; Sarkisov, L. Performance-Based Screening of Porous Materials for Carbon Capture. *Chem. Rev.* **2021**, *121* (17), 10666−10741.
(19) Siegelman, R. L.; Kim, E. J.; Long, J. R. Porous Materials for Carbon Dioxide Separations. *Nat. Mater.* **2021**, *20* (8), 1060−1072.
(20) Wilcox, J.; Haghpanah, R.; Rupp, E. C.; He, J.; Lee, K. Advancing Adsorption and Membrane Separation Processes for the Gigaton Carbon Capture Challenge. *Annu. Rev. Chem. Biomol. Eng.* **2014**, *5* (1), 479−505.
(21) Wu, Y.; Weckhuysen, B. M. Separation and Purification of Hydrocarbons with Porous Materials. *Angew. Chem., Int. Ed.* **2021**, *60* (35), 18930−18949.
(22) Yang, Y.; Bai, P.; Guo, X. Separation of Xylene Isomers: A Review of Recent Advances in Materials. *Ind. Eng. Chem. Res.* **2017**, *56* (50), 14725−14753.
(23) Bao, Z.; Chang, G.; Xing, H.; Krishna, R.; Ren, Q.; Chen, B. Potential of Microporous Metal−Organic Frameworks for Separation of Hydrocarbon Mixtures. *Energy Environ. Sci.* **2016**, *9* (12), 3612−3641.
(24) Smith, A. R.; Klosek, J. A Review of Air Separation Technologies and Their Integration with Energy Conversion Processes. *Fuel Process. Technol.* **2001**, *70* (2), 115−134.
(25) Vinson, D. R. Air Separation Control Technology. *Comput. Chem. Eng.* **2006**, *30* (10), 1436−1446.
(26) *New Developments in Adsorption/Separation of Small Molecules by Zeolites*; Valencia, S., Rey, F., Eds.; Structure and Bonding; Springer International Publishing: Cham, 2020; Vol. *184*. DOI: 10.1007/978-3-030-63853-5.
(27) Shen, Y.; Niu, Z.; Zhang, R.; Zhang, D. Vacuum Pressure Swing Adsorption Process with Carbon Molecular Sieve for CO2 Separation from Biogas. *Journal of CO2 Utilization* **2021**, *54*, 101764.
(28) Ferreira, D.; Boaventura, M.; Barcia, P.; Whitley, R. D.; Mendes, A. Two-Stage Vacuum Pressure Swing Adsorption Using AgLiLSX Zeolite for Producing 99.5+% Oxygen from Air. *Ind. Eng. Chem. Res.* **2016**, *55* (3), 722−736.
(29) Marcinek, A.; Guderian, J.; Bathen, D. Process Intensification of the High-Purity Nitrogen Production in Twin-Bed Pressure Swing Adsorption Plants. *Adsorption* **2021**, *27* (6), 937−952.
(30) Nandanwar, S. U.; Corbin, D. R.; Shiflett, M. B. A Review of Porous Adsorbents for the Separation of Nitrogen from Natural Gas. *Ind. Eng. Chem. Res.* **2020**, *59* (30), 13355−13369.
(31) Kärger, J.; Ruthven, D. M. *Diffusion in zeolites and other microporous solids*; John Wiley & Sons, Inc.: New York, 1992.
(32) Pérez-Botella, E.; Valencia, S.; Rey, F. Zeolites in Adsorption Processes: State of the Art and Future Prospects. *Chem. Rev.* **2022**, *122* (24), 17647−17695.

(33) Sircar, S.; Golden, T. C.; Rao, M. B. Activated Carbon for Gas Separation and Storage. *Carbon* **1996**, *34* (1), 1−12.
(34) Reid, C. R.; O'koy, I. P.; Thomas, K. M. Adsorption of Gases on Carbon Molecular Sieves Used for Air Separation. *Spherical Adsorptives as Probes for Kinetic Selectivity*. *Langmuir* **1998**, *14* (9), 2415−2425.
(35) Wang, Y.; Zhao, D. Beyond Equilibrium: Metal−Organic Frameworks for Molecular Sieving and Kinetic Gas Separation. *Cryst. Growth Des.* **2017**, *17* (5), 2291−2308.
(36) Li, J.-R.; Kuppler, R. J.; Zhou, H.-C. Selective Gas Adsorption and Separation in Metal−Organic Frameworks. *J. Chemical Society Reviews* **2009**, *38* (5), 1477−1504.
(37) Dutcher, B.; Fan, M.; Russell, A. G. Amine-Based CO2 Capture Technology Development from the Beginning of 2013—A Review. *ACS Appl. Mater. Interfaces* **2015**, *7* (4), 2137−2148.
(38) Dawson, R.; Cooper, A. I.; Adams, D. J. Nanoporous Organic Polymer Networks. *Prog. Polym. Sci.* **2012**, *37* (4), 530−563.
(39) Ruthven, D. M. *Principles of Adsorption and Adsorption Processes*; Wiley-Interscience: 1984.
(40) Akhtar, F.; Andersson, L.; Ogunwumi, S.; Hedin, N.; Bergström, L. Structuring Adsorbents and Catalysts by Processing of Porous Powders. *Journal of the European Ceramic Society* **2014**, *34* (7), 1643−1666.
(41) DeWitt, S. J. A.; Sinha, A.; Kalyanaraman, J.; Zhang, F.; Realff, M. J.; Lively, R. P. Critical Comparison of Structured Contactors for Adsorption-Based Gas Separations. *Annu. Rev. Chem. Biomol. Eng.* **2018**, *9* (1), 129−152.
(42) Gueudré, L.; Jolimaître, E.; Bats, N.; Dong, W. Diffusion in Zeolites: Is Surface Resistance a Critical Parameter ? *Adsorption* **2010**, *16* (1), 17−27.
(43) Hibbe, F.; Chmelik, C.; Heinke, L.; Pramanik, S.; Li, J.; Ruthven, D. M.; Tzoulaki, D.; Kärger, J. The Nature of Surface Barriers on Nanoporous Solids Explored by Microimaging of Transient Guest Distributions. *J. Am. Chem. Soc.* **2011**, *133* (9), 2804−2807.
(44) Sastre, G.; Kärger, J.; Ruthven, D. M. Surface Barriers and Symmetry of Adsorption and Desorption Processes. *Adsorption* **2021**, *27* (5), 777−785.
(45) Do, D. D. Adsorption Analysis: Equilibria and Kinetics; Imperial College Press: 1998.
(46) Ruthven, D. M.; Kärger, J.; Theodorou, D. N. *Diffusion in Nanoporous Materials*; John Wiley & Sons: 2012.
(47) Karger, J.; Ruthven, D. M. Diffusion in Nanoporous Materials: Fundamental Principles, Insights and Challenges. *New Journal of Chemistry* **2016**, *40* (5), 4027−4048.
(48) Kärger, J.; Ruthven, D. M.; Valiullin, R. Diffusion in Nanopores: Inspecting the Grounds. *Adsorption* **2021**, *27* (3), 267−281.
(49) Boyd, P. G.; Chidambaram, A.; García-Díez, E.; Ireland, C. P.; Daff, T. D.; Bounds, R.; Gładysiak, A.; Schouwink, P.; Moosavi, S. M.; Maroto-Valer, M. M.; Reimer, J. A.; Navarro, J. A. R.; Woo, T. K.; Garcia, S.; Stylianou, K. C.; Smit, B. Data-Driven Design of Metal−Organic Frameworks for Wet Flue Gas CO2 Capture. *Nature* **2019**, *576* (7786), 253−256.
(50) Rezaei, F.; Webley, P. Structured Adsorbents in Gas Separation Processes. *Sep. Purif. Technol.* **2010**, *70* (3), 243−256.
(51) Krishna, R. Metrics for Evaluation and Screening of Metal−Organic Frameworks for Applications in Mixture Separations. *ACS Omega* **2020**, *5* (28), 16987−17004.
(52) Skoulidas, A. I.; Sholl, D. S. Self-Diffusion and Transport Diffusion of Light Gases in Metal-Organic Framework Materials Assessed Using Molecular Dynamics Simulations. *J. Phys. Chem. B* **2005**, *109* (33), 15760−15768.
(53) Sumida, K.; Rogow, D. L.; Mason, J. A.; McDonald, T. M.; Bloch, E. D.; Herm, Z. R.; Bae, T.-H.; Long, J. R. Carbon Dioxide Capture in Metal−Organic Frameworks. *Chem. Rev.* **2012**, *112* (2), 724−781.
(54) Nugent, P.; Belmabkhout, Y.; Burd, S. D.; Cairns, A. J.; Luebke, R.; Forrest, K.; Pham, T.; Ma, S.; Space, B.; Wojtas, L.; Eddaoudi, M.; Zaworotko, M. J. Porous Materials with Optimal Adsorption Thermodynamics and Kinetics for CO2 Separation. *Nature* **2013**, *495* (7439), 80−84.
(55) Siegelman, R. L.; Kim, E. J.; Long, J. R. Porous Materials for Carbon Dioxide Separations. *Nat. Mater.* **2021**, *20* (8), 1060−1072.
(56) Patankar, S.; Gautam, S.; Rother, G.; Podlesnyak, A.; Ehlers, G.; Liu, T.; Cole, D. R.; Tomasko, D. L. Role of Confinement on Adsorption and Dynamics of Ethane and an Ethane−CO2Mixture in Mesoporous CPG Silica. *J. Phys. Chem. C* **2016**, *120* (9), 4843−4853.
(57) Mo, Y. W.; Kleiner, J.; Webb, M. B.; Lagally, M. G. Activation Energy for Surface Diffusion of Si on Si(001): A Scanning-Tunneling-Microscopy Study. *Phys. Rev. Lett.* **1991**, *66* (15), 1998−2001.
(58) Sharp, C. H.; Bukowski, B. C.; Li, H.; Johnson, E. M.; Ilic, S.; Morris, A. J.; Gersappe, D.; Snurr, R. Q.; Morris, J. R. Nanoconfinement and Mass Transport in Metal−Organic Frameworks. *Chem. Soc. Rev.* **2021**, *50* (20), 11530−11558.
(59) Bousige, C.; Levitz, P.; Coasne, B. Bridging Scales in Disordered Porous Media by Mapping Molecular Dynamics onto Intermittent Brownian Motion. *Nat. Commun.* **2021**, *12* (1), 1043.
(60) Zhu, J.; Liu, J.; Machain, Y.; Bonnett, B.; Lin, S.; Cai, M.; Kessinger, M. C.; Usov, P. M.; Xu, W.; Senanayake, S. D.; Troya, D.; Esker, A. R.; Morris, A. J. Insights into CO2 Adsorption and Chemical Fixation Properties of VPI-100 Metal−Organic Frameworks. *J. Mater. Chem. A* **2018**, *6* (44), 22195−22203.
(61) Grissom, T. G.; Sharp, C. H.; Usov, P. M.; Troya, D.; Morris, A. J.; Morris, J. R. Benzene, Toluene, and Xylene Transport through UiO-66: Diffusion Rates, Energetics, and the Role of Hydrogen Bonding. *J. Phys. Chem. C* **2018**, *122* (28), 16060−16069.
(62) Falk, K.; Coasne, B.; Pellenq, R.; Ulm, F.-J.; Bocquet, L. Subcontinuum Mass Transport of Condensed Hydrocarbons in Nanoporous Media. *Nat. Commun.* **2015**, *6* (1), 6949.
(63) Bocquet, L.; Charlaix, E. Nanofluidics, from Bulk to Interfaces. *Chem. Soc. Rev.* **2010**, *39* (3), 1073−1095.
(64) Ruthven, D. M.; Kärger, J.; Theodorou, D. N. *Diffusion in Nanoporous Materials*; John Wiley & Sons: 2012.
(65) Kärger, J.; Binder, T.; Chmelik, C.; Hibbe, F.; Krautscheid, H.; Krishna, R.; Weitkamp, J. Microimaging of Transient Guest Profiles to Monitor Mass Transfer in Nanoporous Materials. *Nat. Mater.* **2014**, *13* (4), 333−343.
(66) Carslaw, H. S.; Jaeger, J. C. *Conduction of heat in solids*, 2nd ed.; Clarendon Press: Oxford, 1959.
(67) Crank, J. *The mathematics of diffusion*; Oxford University Press: 1979.
(68) Yang, R. T. *Gas separation by adsorption processes*, vol. *1*; World Scientific: 1997. DOI: 10.1142/p037
(69) Glueckauf, E. Theory of Chromatography.Theory of chromatography. Part 10.—Formulæ for diffusion into spheres and their application to chromatography. *Trans. Faraday Soc.* **1955**, *51* (0), 1540−1551.
(70) Krishna, R. A Maxwell-Stefan-Glueckauf Description of Transient Mixture Uptake in Microporous Adsorbents. *Sep. Purif. Technol.* **2018**, *191*, 392−399.
(71) Sircar, S.; Hufton, J. R. Why Does the Linear Driving Force Model for Adsorption Kinetics Work? *Adsorption* **2000**, *6* (2), 137−147.
(72) Krishna, R. Highlighting the Influence of Thermodynamic Coupling on Kinetic Separations with Microporous Crystalline Materials. *ACS Omega* **2019**, *4* (2), 3409−3419.
(73) Krishna, R. Maxwell-Stefan Modelling of Mixture Desorption Kinetics in Microporous Crystalline Materials. *Sep. Purif. Technol.* **2019**, *229*, 115790.
(74) Kärger, J. The Random Walk of Understanding Diffusion. *Ind. Eng. Chem. Res.* **2002**, *41* (14), 3335−3340.
(75) Heinke, L. Diffusion and Photoswitching in Nanoporous Thin Films of Metal-Organic Frameworks. *J. Phys. D: Appl. Phys.* **2017**, *50* (19), 193004.
(76) Chmelik, C.; Kärger, J. In Situ Study on Molecular Diffusion Phenomena in Nanoporous Catalytic Solids. *Chem. Soc. Rev.* **2010**, *39* (12), 4864.

https://doi.org/10.1021/jacs.4c03086
J. Am. Chem. Soc. XXXX, XXX, XXX−XXX

(77) Kruteva, M. Dynamics Studied by Quasielastic Neutron Scattering (QENS). *Adsorption* **2021**, *27* (5), 875−889.
(78) Heinke, L.; Chmelik, C.; Kortunov, P.; Ruthven, D. M.; Shah, D. B.; Vasenkov, S.; Kärger, J. Application of Interference Microscopy and IR Microscopy for Characterizing and Investigating Mass Transport in Nanoporous Materials. *Chem. Eng. Technol.* **2007**, *30* (8), 995−1002.
(79) Kärger, J.; Chmelik, C.; Heinke, L.; Valiullin, R. A New View of Diffusion in Nanoporous Materials. *Chemie Ingenieur Technik* **2010**, *82* (6), 779−804.
(80) Kärger, J.; Binder, T.; Chmelik, C.; Hibbe, F.; Krautscheid, H.; Krishna, R.; Weitkamp, J. Microimaging of Transient Guest Profiles to Monitor Mass Transfer in Nanoporous Materials. *Nat. Mater.* **2014**, *13* (4), 333−343.
(81) Gaikwad, S.; Kim, S.-J.; Han, S. Novel Metal−Organic Framework of UTSA-16 (Zn) Synthesized by a Microwave Method: Outstanding Performance for CO2 Capture with Improved Stability to Acid Gases. *Journal of Industrial and Engineering Chemistry* **2020**, *87*, 250−263.
(82) Wang, J.-Y.; Mangano, E.; Brandani, S.; Ruthven, D. M. A Review of Common Practices in Gravimetric and Volumetric Adsorption Kinetic Experiments. *Adsorption* **2021**, *27* (3), 295−318.
(83) Brandani, S.; Mangano, E. The Zero Length Column Technique to Measure Adsorption Equilibrium and Kinetics: Lessons Learnt from 30 Years of Experience. *Adsorption* **2021**, *27* (3), 319−351.
(84) Wang, Y. Identification of Mass Transfer Resistances in Microporous Materials Using Frequency Response Methods. *Adsorption* **2021**, *27* (3), 369−395.
(85) Wilkins, N. S.; Rajendran, A.; Farooq, S. Dynamic Column Breakthrough Experiments for Measurement of Adsorption Equilibrium and Kinetics. *Adsorption* **2021**, *27* (3), 397−422.
(86) Silva, J. A. C.; Rodrigues, A. E. Limitations of the Zero-Length Column Technique to Measure Diffusional Time Constants in Microporous Adsorbents. *Chem. Eng. Technol.* **2015**, *38* (12), 2335−2339.
(87) Karge, H. G.; Weitkamp, J. *Adsorption and Diffusion*; Springer Science & Business Media: 2008.
(88) Chmelik, C.; Gläser, R.; Haase, J.; Hwang, S.; Kärger, J. Application of Microimaging to Diffusion Studies in Nanoporous Materials. *Adsorption* **2021**, *27* (5), 819−840.
(89) Heinke, L.; Kortunov, P.; Tzoulaki, D.; Kärger, J. The Options of Interference Microscopy to Explore the Significance of Intracrystalline Diffusion and Surface Permeation for Overall Mass Transfer on Nanoporous Materials. *Adsorption* **2007**, *13* (3), 215−223.
(90) Xiang, W.; Zhang, Y.; Chen, Y.; Liu, C.; Tu, X. Synthesis, Characterization and Application of Defective Metal−Organic Frameworks: Current Status and Perspectives. *Journal of Materials Chemistry A* **2020**, *8* (41), 21526−21546.
(91) Iacomi, P.; Formalik, F.; Marreiros, J.; Shang, J.; Rogacka, J.; Mohmeyer, A.; Behrens, P.; Ameloot, R.; Kuchta, B.; Llewellyn, P. L. Role of Structural Defects in the Adsorption and Separation of C3 Hydrocarbons in Zr-Fumarate-MOF (MOF-801). *Chem. Mater.* **2019**, *31* (20), 8413−8423.
(92) Han, C.; Verploegh, R. J.; Sholl, D. S. Assessing the Impact of Point Defects on Molecular Diffusion in ZIF-8 Using Molecular Simulations. *J. Phys. Chem. Lett.* **2018**, *9* (14), 4037−4044.
(93) Tanaka, S.; Fujita, K.; Miyake, Y.; Miyamoto, M.; Hasegawa, Y.; Makino, T.; Van der Perre, S.; Cousin Saint Remi, J.; Van Assche, T.; Baron, G. V.; Denayer, J. F. M. Adsorption and Diffusion Phenomena in Crystal Size Engineered ZIF-8 MOF. *The Journal of Physical Chemistry C* **2015**, *119* (51), 28430−28439.
(94) Remi, J. C. S.; Lauerer, A.; Chmelik, C.; Vandendael, I.; Terryn, H.; Baron, G. V.; Denayer, J. F. M.; Kärger, J. The Role of Crystal Diversity in Understanding Mass Transfer in Nanoporous Materials. *Nat. Mater.* **2016**, *15* (4), 401−406.
(95) Hu, X.; Mangano, E.; Friedrich, D.; Ahn, H.; Brandani, S. Diffusion Mechanism of CO2 in 13X Zeolite Beads. *Adsorption* **2014**, *20* (1), 121−135.
(96) Kamiuto, K.; Goubaru, A.; Ermalina. Diffusion Coefficients of Carbon Dioxide Within Type 13x Zeolite Particles. *Chemical Engineering Communications* **2006**, *193* (5), 628−638.
(97) *Project Details Diffusion in nanoporous solids*. IUPAC | International Union of Pure and Applied Chemistry. https://iupac.org/project/2015-002-2-100 (accessed 2024-02-15).
(98) Kärger, J.; Vasenkov, S. Quantitation of Diffusion in Zeolite Catalysts. *Microporous Mesoporous Mater.* **2005**, *85* (3), 195−206.
(99) Alder, B. J.; Wainwright, T. E. Studies in Molecular Dynamics. *II. Behavior of a Small Number of Elastic Spheres. The Journal of Chemical Physics* **1960**, *33* (5), 1439−1451.
(100) Frentrup, H.; Avendano, C.; Horsch, M.; Salih, A.; Muller, E. A. Transport Diffusivities of Fluids in Nanopores by Non-Equilibrium Molecular Dynamics Simulation. *Mol. Simul.* **2012**, *38* (7), 540−553.
(101) Beerdsen, E.; Smit, B.; Dubbeldam, D. Molecular Simulation of Loading Dependent Slow Diffusion in Confined Systems. *Phys. Rev. Lett.* **2004**, *93* (24), 248301.
(102) Bukowski, B. C.; Keil, F. J.; Ravikovitch, P. I.; Sastre, G.; Snurr, R. Q.; Coppens, M.-O. Connecting Theory and Simulation with Experiment for the Study of Diffusion in Nanoporous Solids. *Adsorption* **2021**, *27* (5), 683−760.
(103) Gibaldi, M.; Kwon, O.; White, A.; Burner, J.; Woo, T. K. The HEALED SBU Library of Chemically Realistic Building Blocks for Construction of Hypothetical Metal−Organic Frameworks. *ACS Appl. Mater. Interfaces* **2022**, *14* (38), 43372−43386.
(104) García-Sánchez, A.; van den Bergh, J.; Castillo, J. M.; Calero, S.; Kapteijn, F.; Vlugt, T. J. H. Influence of Force Field Parameters on Computed Diffusion Coefficients of CO2 in LTA-Type Zeolite. *Microporous Mesoporous Mater.* **2012**, *158*, 64−76.
(105) Yang, Y.; Yu, Z.; Sholl, D. S. Machine Learning Models for Predicting Molecular Diffusion in Metal−Organic Frameworks Accounting for the Impact of Framework Flexibility. *Chem. Mater.* **2023**, *35* (23), 10156−10168.
(106) García-Sánchez, A.; Dubbeldam, D.; Calero, S. Modeling Adsorption and Self-Diffusion of Methane in LTA Zeolites: The Influence of Framework Flexibility. *J. Phys. Chem. C* **2010**, *114* (35), 15068−15074.
(107) Park, H.; Yan, X.; Zhu, R.; Huerta, E. A.; Chaudhuri, S.; Cooper, D.; Foster, I.; Tajkhorshid, E. A Generative Artificial Intelligence Framework Based on a Molecular Diffusion Model for the Design of Metal-Organic Frameworks for Carbon Capture. *Commun. Chem.* **2024**, *7* (1), 1−18.
(108) Jee, S. E.; Sholl, D. S. Carbon Dioxide and Methane Transport in DDR Zeolite: Insights from Molecular Simulations into Carbon Dioxide Separations in Small Pore Zeolites. *J. Am. Chem. Soc.* **2009**, *131* (22), 7896−7904.
(109) Hedin, N.; DeMartin, G. J.; Roth, W. J.; Strohmaier, K. G.; Reyes, S. C. PFG NMR Self-Diffusion of Small Hydrocarbons in High Silica DDR, CHA and LTA Structures. *Microporous Mesoporous Mater.* **2008**, *109* (1), 327−334.
(110) Binder, T.; Chmelik, C.; Kärger, J.; Martinez-Joaristi, A.; Gascon, J.; Kapteijn, F.; Ruthven, D. A Diffusion Study of Small Hydrocarbons in DDR Zeolites by Micro-Imaging. *Microporous Mesoporous Mater.* **2013**, *180*, 219−228.
(111) Vidoni, A.; Ruthven, D. Diffusion of Methane in DD3R Zeolite. *Microporous Mesoporous Mater.* **2012**, *159*, 57−65.
(112) Bukowski, B. C.; Snurr, R. Q. Topology-Dependent Alkane Diffusion in Zirconium Metal−Organic Frameworks. *ACS Appl. Mater. Interfaces* **2020**, *12* (50), 56049−56059.
(113) Forse, A. C.; Colwell, K. A.; Gonzalez, M. I.; Benders, S.; Torres-Gavosto, R. M.; Blümich, B.; Reimer, J. A.; Long, J. R. Influence of Pore Size on Carbon Dioxide Diffusion in Two Isoreticular Metal−Organic Frameworks. *Chem. Mater.* **2020**, *32* (8), 3570−3576.
(114) Magnin, Y.; Dirand, E.; Maurin, G.; Llewellyn, P. L. Abnormal CO2 and H2O Diffusion in CALF-20(Zn) Metal−Organic Frame-

https://doi.org/10.1021/jacs.4c03086
J. Am. Chem. Soc. XXXX, XXX, XXX−XXX

work: Fundamental Understanding of CO2 Capture. *ACS Appl. Nano Mater.* **2023**, *6* (21), 19963−19971.
(115) Krishna, R.; van Baten, J. M. Insights into Diffusion of Gases in Zeolites Gained from Molecular Dynamics Simulations. *Microporous Mesoporous Mater.* **2008**, *109* (1), 91−108.
(116) Krishna, R.; van Baten, J. M. A Molecular Dynamics Investigation of a Variety of Influences of Temperature on Diffusion in Zeolites. *Microporous Mesoporous Mater.* **2009**, *125* (1), 126−134.
(117) Newsome, D.; Coppens, M.-O. Molecular Dynamics as a Tool to Study Heterogeneity in Zeolites − Effect of Na+ Cations on Diffusion of CO2 and N2 in Na-ZSM-5. *Chem. Eng. Sci.* **2015**, *121*, 300−312.
(118) Yang, Q.; Wiersum, A. D.; Jobic, H.; Guillerm, V.; Serre, C.; Llewellyn, P. L.; Maurin, G. Understanding the Thermodynamic and Kinetic Behavior of the CO2/CH4 Gas Mixture within the Porous Zirconium Terephthalate UiO-66(Zr): A Joint Experimental and Modeling Approach. *J. Phys. Chem. C* **2011**, *115* (28), 13768−13774.
(119) Krishna, R.; van Baten, J. M.; García-Pérez, E.; Calero, S. Diffusion of CH4 and CO2 in MFI, CHA and DDR Zeolites. *Chem. Phys. Lett.* **2006**, *429* (1), 219−224.
(120) Krishna, R.; van Baten, J. M. Insights into Diffusion of Gases in Zeolites Gained from Molecular Dynamics Simulations. *Microporous Mesoporous Mater.* **2008**, *109* (1), 91−108.
(121) Krishna, R.; van Baten, J. M. Segregation Effects in Adsorption of CO2-Containing Mixtures and Their Consequences for Separation Selectivities in Cage-Type Zeolites. *Sep. Purif. Technol.* **2008**, *61* (3), 414−423.
(122) Tsimpanogiannis, I. N.; Moultos, O. A.; Franco, L. F. M.; Spera, M. B. de M.; Erdős, M.; Economou, I. G. Self-Diffusion Coefficient of Bulk and Confined Water: A Critical Review of Classical Molecular Simulation Studies. *Mol. Simul.* **2019**, *45* (4−5), 425−453.
(123) Formalik, F.; Shi, K.; Joodaki, F.; Wang, X.; Snurr, R. Q. Exploring the Structural, Dynamic, and Functional Properties of Metal-Organic Frameworks through Molecular Modeling. *Advanced Functional Materials* **2023**, 2308130.
(124) Sharp, C. H.; Bukowski, B. C.; Li, H.; Johnson, E. M.; Ilic, S.; Morris, A. J.; Gersappe, D.; Snurr, R. Q.; Morris, J. R. Nanoconfinement and Mass Transport in Metal−Organic Frameworks. *Chem. Soc. Rev.* **2021**, *50* (20), 11530−11558.
(125) Boţan, A.; Ulm, F.-J.; Pellenq, R. J.-M.; Coasne, B. Bottom-up Model of Adsorption and Transport in Multiscale Porous Media. *Phys. Rev. E* **2015**, *91* (3), No. 032133.
(126) Apostolopoulou, M.; Stamatakis, M.; Striolo, A.; Dusterhoft, R.; Hull, R.; Day, R. A Novel Modeling Approach to Stochastically Evaluate the Impact of Pore Network Geometry, Chemistry and Topology on Fluid Transport. *Transp Porous Med.* **2021**, *136* (2), 495−520.
(127) He, Y.-L.; Tao, W.-Q. Numerical Solutions of Nano/Microphenomena Coupled With Macroscopic Process of Heat Transfer and Fluid Flow: A Brief Review. *Journal of Heat Transfer* **2015**, *137*, 090801.
(128) Thomas, A. M.; Subramanian, Y. Simulations on "Powder" Samples for Better Agreement with Macroscopic Measurements. *J. Phys. Chem. C* **2019**, *123* (26), 16172−16178.
(129) Rezaei, F.; Webley, P. Structured Adsorbents in Gas Separation Processes. *Sep. Purif. Technol.* **2010**, *70* (3), 243−256.
(130) Rezaei, F.; Webley, P. A. Optimal Design of Engineered Gas Adsorbents: Pore-Scale Level. *Chem. Eng. Sci.* **2012**, *69* (1), 270−278.
(131) Hasan, F. A.; Xiao, P.; Singh, R. K.; Webley, P. A. Zeolite Monoliths with Hierarchical Designed Pore Network Structure: Synthesis and Performance. *Chemical Engineering Journal* **2013**, *223*, 48−58.
(132) Lawson, S.; Li, X.; Thakkar, H.; Rownaghi, A. A.; Rezaei, F. Recent Advances in 3D Printing of Structured Materials for Adsorption and Catalysis Applications. *Chem. Rev.* **2021**, *121* (10), 6246−6291.
(133) Chen, L.-H.; Sun, M.-H.; Wang, Z.; Yang, W.; Xie, Z.; Su, B.-L. Hierarchically Structured Zeolites: From Design to Application. *Chem. Rev.* **2020**, *120* (20), 11194−11294.
(134) Chmelik, C.; Caro, J.; Freude, D.; Haase, J.; Valiullin, R.; Kärger, J. Diffusive Spreading of Molecules in Nanoporous Materials. In *Diffusive Spreading in Nature, Technology and Society;* Bunde, A., Caro, J., Chmelik, C., Kärger, J., Vogl, G., Eds.; Springer International Publishing: Cham, 2023; pp 179−214. DOI: 10.1007/978-3-031-05946-9_10.
(135) Onyestyák, G.; Shen, D.; Rees, L. V. C. Frequency-Response Studies of CO2 Diffusion in Commercial 5A Powders and Pellets. *Microporous Materials* **1996**, *5* (5), 279−288.
(136) Sircar, S. Adsorbate Mass Transfer into Porous Adsorbents − A Practical Viewpoint. *Sep. Purif. Technol.* **2018**, *192*, 383−400.
(137) Diffusion Mechanisms. In *Diffusion in Nanoporous Materials*; John Wiley & Sons, Ltd: 2012; pp 85−110. DOI: 10.1002/9783527651276.ch4.
(138) Roque-Malherbe, R. M. A. *Adsorption and Diffusion in Nanoporous Materials (1st ed.)*; CRC Press: 2007. DOI: 10.1201/9781420046762.
(139) Gardner, T. Q.; Ruthven, D. M.; Conner, Wm. C.; Fraissard, J. NATO-ASI Fluid Transport in Nanoporous Materials Course.a Student's Perspective and Explanations from a Veteran NATO Science Series II: Mathematics Physics and Chemistry. *Fluid Transport in Nanoporous Materials* **2006**, *219*, 1−7.
(140) Kolle, J. M.; Fayaz, M.; Sayari, A. Understanding the Effect of Water on CO2 Adsorption. *Chem. Rev.* **2021**, *121* (13), 7280−7345.
(141) Chanut, N.; Bourrelly, S.; Kuchta, B.; Serre, C.; Chang, J.-S.; Wright, P. A.; Llewellyn, P. L. Screening the Effect of Water Vapour on Gas Adsorption Performance: Application to CO2 Capture from Flue Gas in Metal−Organic Frameworks. *ChemSusChem* **2017**, *10* (7), 1543−1553.
(142) Soubeyrand-Lenoir, E.; Vagner, C.; Yoon, J. W.; Bazin, P.; Ragon, F.; Hwang, Y. K.; Serre, C.; Chang, J.-S.; Llewellyn, P. L. How Water Fosters a Remarkable 5-Fold Increase in Low-Pressure CO2 Uptake within Mesoporous MIL-100(Fe). *J. Am. Chem. Soc.* **2012**, *134* (24), 10174−10181.
(143) Yazaydın, A. Ö.; Benin, A. I.; Faheem, S. A.; Jakubczak, P.; Low, J. J.; Willis, R. R.; Snurr, R. Q. Enhanced CO2 Adsorption in Metal-Organic Frameworks via Occupation of Open-Metal Sites by Coordinated Water Molecules. *Chem. Mater.* **2009**, *21* (8), 1425−1430.
(144) Benoit, V.; Chanut, N.; Pillai, R. S.; Benzaqui, M.; Beurroies, I.; Devautour-Vinot, S.; Serre, C.; Steunou, N.; Maurin, G.; Llewellyn, P. L. A Promising Metal−Organic Framework (MOF), MIL-96(Al), for CO2 Separation under Humid Conditions. *J. Mater. Chem. A* **2018**, *6* (5), 2081−2090.
(145) Rajendran, A.; Shimizu, G. K. H.; Woo, T. K. The Challenge of Water Competition in Physical Adsorption of CO2 by Porous Solids for Carbon Capture Applications − A Short Perspective. *Adv. Mater.* **2024**, *36* (12), 2301730.
(146) Polat, H. M.; Coelho, F. M.; Vlugt, T. J. H.; Mercier Franco, L. F.; Tsimpanogiannis, I. N.; Moultos, O. A. Diffusivity of CO_2 in H_2O: A Review of Experimental Studies and Molecular Simulations in the Bulk and in Confinement. *J. Chem. Eng. Data* **2024**. DOI: 10.1021/acs.jced.3c00778.
(147) Hunvik, K. W. B.; Lima, R. J. da S.; Kirch, A.; Loch, P.; Monceyron Røren, P.; Hoffmann Petersen, M.; Rudić, S.; García Sakai, V.; Knudsen, K. D.; Rodrigues Miranda, C.; Breu, J.; Fossum, J. O.; Bordallo, H. N. Influence of CO2 on Nanoconfined Water in a Clay Mineral. *J. Phys. Chem. C* **2022**, *126* (40), 17243−17254.
(148) Magnin, Y.; Dirand, E.; Orsikowsky, A.; Plainchault, M.; Pugnet, V.; Cordier, P.; Llewellyn, P. L. A Step in Carbon Capture from Wet Gases: Understanding the Effect of Water on CO2 Adsorption and Diffusion in UiO-66. *J. Phys. Chem. C* **2022**, *126* (6), 3211−3220.
(149) Bendt, S.; Dong, Y.; Keil, F. J. Diffusion of Water and Carbon Dioxide and Mixtures Thereof in Mg-MOF-74. *J. Phys. Chem. C* **2019**, *123* (13), 8212−8220.

https://doi.org/10.1021/jacs.4c03086
J. Am. Chem. Soc. XXXX, XXX, XXX−XXX

(150) Mera, H. A.; Gomez-Ballesteros, J. L.; Balbuena, P. B. Structure and Dynamics of Carbon Dioxide, Nitrogen, Water, and Their Mixtures in Metal Organic Frameworks. *J. Chem. Eng. Data* **2014**, *59* (10), 2973−2981.
(151) Rochelle, G. T. Amine Scrubbing for CO2 Capture. *Science* **2009**, *325* (5948), 1652−1654.
(152) Belmabkhout, Y.; Serna-Guerrero, R.; Sayari, A. Amine-Bearing Mesoporous Silica for CO2 Removal from Dry and Humid Air. *Chem. Eng. Sci.* **2010**, *65* (11), 3695−3698.
(153) Choi, S.; Drese, J. H.; Eisenberger, P. M.; Jones, C. W. Application of Amine-Tethered Solid Sorbents for Direct CO2 Capture from the Ambient Air. *Environ. Sci. Technol.* **2011**, *45* (6), 2420−2427.
(154) Pang, S. H.; Jue, M. L.; Leisen, J.; Jones, C. W.; Lively, R. P. PIM-1 as a Solution-Processable "Molecular Basket" for CO2 Capture from Dilute Sources. *ACS Macro Lett.* **2015**, *4* (12), 1415−1419.
(155) Wang, J.; Wang, M.; Zhao, B.; Qiao, W.; Long, D.; Ling, L. Mesoporous Carbon-Supported Solid Amine Sorbents for Low-Temperature Carbon Dioxide Capture. *Ind. Eng. Chem. Res.* **2013**, *52* (15), 5437−5444.
(156) McDonald, T. M.; Lee, W. R.; Mason, J. A.; Wiers, B. M.; Hong, C. S.; Long, J. R. Capture of Carbon Dioxide from Air and Flue Gas in the Alkylamine-Appended Metal−Organic Framework Mmen-Mg2(Dobpdc). *J. Am. Chem. Soc.* **2012**, *134* (16), 7056−7065.
(157) Yu, J.; Chuang, S. S. C. The Structure of Adsorbed Species on Immobilized Amines in CO2 Capture: An in Situ IR Study. *Energy Fuels* **2016**, *30* (9), 7579−7587.
(158) Kuwahara, Y.; Kang, D.-Y.; Copeland, J. R.; Brunelli, N. A.; Didas, S. A.; Bollini, P.; Sievers, C.; Kamegawa, T.; Yamashita, H.; Jones, C. W. Dramatic Enhancement of CO2 Uptake by Poly(Ethyleneimine) Using Zirconosilicate Supports. *J. Am. Chem. Soc.* **2012**, *134* (26), 10757−10760.
(159) Stuckert, A. N.; Yang, R. T. CO2 Capture from the Atmosphere and Simultaneous Concentration Using Zeolites and Amine-Grafted SBA-15. *Environ. Sci. Technol.* **2011**, *45* (23), 10257−10264.
(160) Veneman, R.; Frigka, N.; Zhao, W.; Li, Z.; Kersten, S.; Brilman, W. Adsorption of H2O and CO2 on Supported Amine Sorbents. *International Journal of Greenhouse Gas Control* **2015**, *41*, 268−275.
(161) Gebald, C.; Wurzbacher, J. A.; Borgschulte, A.; Zimmermann, T.; Steinfeld, A. Single-Component and Binary CO2 and H2O Adsorption of Amine-Functionalized Cellulose. *Environ. Sci. Technol.* **2014**, *48* (4), 2497−2504.
(162) Mason, J. A.; McDonald, T. M.; Bae, T.-H.; Bachman, J. E.; Sumida, K.; Dutton, J. J.; Kaye, S. S.; Long, J. R. Application of a High-Throughput Analyzer in Evaluating Solid Adsorbents for Post-Combustion Carbon Capture via Multicomponent Adsorption of CO2, N2, and H2O. *J. Am. Chem. Soc.* **2015**, *137* (14), 4787−4803.
(163) Young, J.; Garcia-Diez, E.; Garcia, S.; van der Spek, M. The Impact of Binary Water−CO 2 Isotherm Models on the Optimal Performance of Sorbent-Based Direct Air Capture Processes. *Energy Environ. Sci.* **2021**, *14* (10), 5377−5394.
(164) McDonald, T. M.; Mason, J. A.; Kong, X.; Bloch, E. D.; Gygi, D.; Dani, A.; Crocellà, V.; Giordanino, F.; Odoh, S. O.; Drisdell, W. S.; Vlaisavljevich, B.; Dzubak, A. L.; Poloni, R.; Schnell, S. K.; Planas, N.; Lee, K.; Pascal, T.; Wan, L. F.; Prendergast, D.; Neaton, J. B.; Smit, B.; Kortright, J. B.; Gagliardi, L.; Bordiga, S.; Reimer, J. A.; Long, J. R. Cooperative Insertion of CO2 in Diamine-Appended Metal-Organic Frameworks. *Nature* **2015**, *519* (7543), 303−308.
(165) Andreoli, E.; Cullum, L.; Barron, A. R. Carbon Dioxide Absorption by Polyethylenimine-Functionalized Nanocarbons: A Kinetic Study. *Ind. Eng. Chem. Res.* **2015**, *54* (3), 878−889.
(166) Sircar, S. Basic Research Needs for Design of Adsorptive Gas Separation Processes. *Ind. Eng. Chem. Res.* **2006**, *45* (16), 5435−5448.
(167) Hu, X.; Brandani, S.; Benin, A. I.; Willis, R. R. Testing the Stability of Novel Adsorbents for Carbon Capture Applications Using the Zero Length Column Technique. *Chem. Eng. Res. Des.* **2018**, *131*, 406−413.
(168) Shade, D.; Bout, B. W. S.; Sholl, D. S.; Walton, K. S. Opening the Toolbox: 18 Experimental Techniques for Measurement of Mixed Gas Adsorption. *Ind. Eng. Chem. Res.* **2022**, *61* (6), 2367−2391.

https://doi.org/10.1021/jacs.4c03086
J. Am. Chem. Soc. XXXX, XXX, XXX−XXX